

# Synthesis of a Novel Highly Efficient Flame-Retardant Coating for Cotton Fabrics With Low Combustion Toxicity and Antibacterial Properties

**Ghada Makhlof**

National Institute of Standards

**aksam abdelkhalik** (✉ [aksamhassan85@gmail.com](mailto:aksamhassan85@gmail.com))

National Institute of Standards

**Heba Ameen**

National Institute of Standards

---

## Research Article

**Keywords:** Tannic acid, flame retardant, cotton fabric, smoke suppression, mechanical properties, antibacterial properties

**Posted Date:** March 22nd, 2021

**DOI:** <https://doi.org/10.21203/rs.3.rs-315407/v1>

**License:**  This work is licensed under a Creative Commons Attribution 4.0 International License.

[Read Full License](#)

---

**Version of Record:** A version of this preprint was published at Cellulose on July 15th, 2021. See the published version at <https://doi.org/10.1007/s10570-021-04076-2>.

# 1 **Synthesis of a novel highly efficient flame-retardant coating for cotton** 2 **fabrics with low combustion toxicity and antibacterial properties**

3  
4 Ghada Makhoul<sup>a</sup>, Aksam Abdelkhalik<sup>a,\*</sup>, Heba Ameen<sup>b</sup>

5  
6 <sup>a</sup>Fire and explosion protection Lab, National Institute of Standards, NIS, Egypt. El Sadaat  
7 street, El-Haram, El-Giza. P.O.Box 136 code 12211

8 <sup>b</sup>Textile Metrology Lab, National Institute of Standards, NIS, Egypt. El Sadaat street, El-  
9 Haram, El-Giza. P.O.Box 136 code 12211

## 10 11 **Abstract**

12 Synthesis of multi-function flame retardants is widely increasing to fulfil industrial and  
13 economic goals. In this work, a novel flame retardant, melamine salt of tannic phosphate  
14 (MTP) was prepared and characterized. MTP was mixed with polyvinyl alcohol (PVA)  
15 solution and used as a coating for cotton fabrics. In addition, tannic acid (TA) and melamine  
16 phosphate (MP) were mixed with PVA solution and applied as a coating for cotton fabrics.  
17 Vertical and horizontal flammability tests showed that the flame did not propagate in samples  
18 treated with PVA/MTP. In contrast, samples treated with PVA/TA/MP burnt completely.  
19 Limiting oxygen index (LOI) data indicated that samples treated with PVA/30%MTP reached  
20 LOI value 68.4%, while control sample had LOI value 17.1%. Smoke density results presented  
21 that PVA/MTP succeeded in reducing the maximum specific optical density ( $D_{s\ max}$ ) of cotton  
22 fabrics. FTIR gas analyzer results manifested that addition of PVA/MTP to cotton fabrics  
23 decreased the emission of CO, CO<sub>2</sub>, C<sub>3</sub>H<sub>8</sub>, C<sub>2</sub>H<sub>6</sub>, C<sub>6</sub>H<sub>14</sub> and formaldehyde in the gas phase.  
24 Fractional effective dose (FED) and lethal toxic potency (LC<sub>50</sub>) showed that samples coated  
25 with PVA/MTP are less toxic than blank. In addition, these fabrics exhibited a remarkable  
26 antibacterial property against gram-positive and gram-negative bacteria.

## 27 28 **Keywords**

29 Tannic acid, flame retardant, cotton fabric, smoke suppression, mechanical properties,  
30 antibacterial properties

31  
32  
33

## 341. Introduction

35 Cotton fabrics are excessively used in applications like clothing and house furniture due to  
36 their fabulous properties which includes comfortableness, biodegradability, hydrophilicity and  
37 good breathability (Chen et al. 2021; Zhu et al. 2020a). However, cotton fabrics are highly  
38 flammable and this problem restricts their industrial applications. For instance, LOI of cotton  
39 fabric is in the range 16-18%, which makes fabrics able to combust at ambient conditions  
40 (where O<sub>2</sub> in air is 20.95%) (Chen et al. 2020). To overcome this problem, many studies gave  
41 great interest to improve the flame retardancy using different kinds of flame retardant  
42 materials. As cotton fabric is naturally occurring material, an after finish method is used to  
43 improve its flame retardancy (Pan et al. 2015). Halogenated flame retardants such as  
44 pentabromodiphenyl ether, decabromodiphenyl ether and (Polychlorinated Biphenyl) showed  
45 good flame retardancy characteristics. However, the environmental regulations in many  
46 countries restricted their use because these materials manifested harmful effects to human and  
47 animals (Van der Veen and De Boer, 2012). Metal hydroxides such as Al(OH)<sub>3</sub> and Mg(OH)<sub>2</sub>  
48 were introduced as alternatives for halogenated flame retardants because they can take in a  
49 large amount of heat at high temperatures. But these materials should be added at high  
50 concentrations to obtain good flame retardancy action. The high loading levels of these  
51 materials deteriorate the mechanical properties (Hu et al. 2020; Zhu et al. 2020b; Laoutid et al.  
52 2009). Intumescent flame retardants (IFRs) were used by many researchers to improve the  
53 flame retardancy of cotton fabrics because they are environmentally friendly (halogen free  
54 compounds) and produce low amounts of smoke and toxic gases (Wang et al. 2021).  
55 Traditional IFRs are consisting of acid source (like phosphoric acid), charring agent (like  
56 pentaerythritol) and bellowing agent (such as melamine). The ingredients of IFR system are  
57 decomposed during the combustion process of polymer composite to form insulating, cellular  
58 and intumescent char layer on polymer surface which protect the polymer from the effect of  
59 heat and flame. Moreover, it reduces the evolving of volatile organic compounds to the  
60 combustion zone (Wang et al. 2021; Chan et al. 2018; Fang et al. 2015). Recently, much  
61 research work was directed to combine the IFRs ingredients in one molecule to reduce the  
62 polarity of traditional IFRs and preparing single molecule intumescent flame retardant  
63 (SMIFR) (Makhlouf et al. 2020; Yang et al. 2019; Jian et al. 2019). In our previous work we  
64 prepared different melamine salts such as melamine salt of montmorillonite phosphate (MMP),  
65 melamine salt of pentaerythritol phosphate montmorillonite (MPPM) and melamine salt of  
66 chitosan phosphate (MCHP) as SMIFR and it showed good flame retardancy action on  
67 polypropylene and polyethylene (Makhlouf et al. 2017a, 2017b; Hassan et al. 2016).

68 Tannic acid (TA) is one of hydrolyzable tannins, commercial available and has an  
69 estimated chemical structure  $C_{76}H_{52}O_{46}$ . It is composed of inner layer containing glucose ring  
70 and outer layers consisting of gallic acid units. TA is used in different industries such as inks,  
71 plastic resins, adhesives, surface coatings and dyes. Besides; it is used in water treatment  
72 process (Das et al. 2020; Ramakrishnan and Krishnan, 1994). Pantoja-Castro and González-  
73 Rodríguez (2011) used the thermogravimetric analysis technique to differentiate between TA  
74 and condensed tannins. The authors reported that tannins were decomposed through three  
75 decomposition steps meanwhile TA showed five decomposition steps. This was referred to that  
76 TA has less complex structure and its bonds may be easily broken to form smaller structures.  
77 Also, the char residue at 600 °C was higher in case of condensed tannins due to tannins have  
78 more carbon atoms in their chemical structure than TA. Pyrolysis of tannins at 600 °C yields  
79 mainly catechol as a peculiar fragment (Nam et al. 2017; Galletti and Reeves, 1992). On the  
80 other hand, TA produces 1,2- benzene diol and 1,2,3-benzene triol from degradation of the  
81 outer layer that containing gallic acid units. The inner layer was characterized by stability to  
82 higher temperatures and at temperature >700 °C, it crosslinked to form intumescent  
83 carbonaceous char (Nam et al. 2017; Xia et al. 2015). Tributsch and Fiechter (2008) stated that  
84 the presence of tannins in the bark of trees makes them naturally fire resistant due to tannins  
85 have antioxidant effects and are able to neutralize radicals through their electron donation  
86 properties. Therefore, tannins seem to be a new bio based materials that can be used in the  
87 development of fire retardant additives (Das et al. 2020; Singh and Kumar, 2020; Nam et al.  
88 2017). Nam et al. (2017) treated cotton fabric with TA and TA/sodium hydroxide solution as  
89 IFR. The authors stated that, in one hand, treating cotton samples with 20% TA alone was able  
90 to alter the combustion behaviour of cotton. Microscale calorimeter results showed that  
91 20%TA decreased the heat release capacity (HRC) of cotton by 35.8% and increased the char  
92 residue from 6.3% to 16.9%. However, TA alone was not sufficient to make improvement in  
93 the LOI value of cotton fabric. On the other hand, when treating cotton fabrics with  
94 20%TA/1% sodium hydroxide LOI value increased to 30.2%, and the HRC of control sample  
95 was reduced by 81.8% and the char residue was increased to 21.5%. But the durability,  
96 mechanical and vertical flammability properties were not studied. According to our literature  
97 survey, combining TA as charring agent with other IFR ingredients to prepare SMIFR to  
98 impart different functions (such as flame retardancy and antibacterial effects) to cotton fabric  
99 was not studied.

100 Fire toxicity is considered the main reason of death and harm from unexpected fires. In the  
101 UK, during the period from 1955 to 2015, there has been a gradual transfer for the reason of

102 death from burn to toxic gases, and the injuries due to fire toxicity increased greatly (Stec,  
 103 2017; Stull, 2008). The exposure to toxic gases (such as CO, CO<sub>2</sub>, NO<sub>x</sub>, SO<sub>2</sub>, acrolein, HCHO,  
 104 NH<sub>3</sub>, HCl and HBr) which are produced from fatal fires drive to set of physiological and  
 105 behavioural effects. For instance, physical incapacitation and loss of sense of direction can take  
 106 place when the person is subjected to these gases, and these effects are likely threat life because  
 107 they can hinder safe escape. In the last decades, chemical analysis (without refuge to  
 108 experiments on animals) was used to predict the main effects for fire toxicity like  
 109 incapacitation by quantifying the toxic gases evolved during different fire conditions in small  
 110 scale tests (Stec, 2017). Fractional Effective Dose (FED) is used in creating toxic potency data  
 111 using chemical analysis of fire effluents, by taking into account the toxic effects of CO, CO<sub>2</sub>,  
 112 HCl, HBr, NO<sub>x</sub>, SO<sub>2</sub>, anoxia and other toxic gases. FED is defined as the ratio of the  
 113 concentration and time product for a toxic gas released in a given test to the concentration and  
 114 time product of that toxicant that has been statistically defined from distinct experimental data  
 115 to cause lethality in 50% of test animals during a fixed exposure and post exposure time (Stec,  
 116 2017; Chow et al.2020). FED was calculated following to Eq. (1) (ISO 13344: 1996); Chow et  
 117 al. 2020).

$$118 \quad \text{FED} = \frac{[\text{CO}]}{5000} + \frac{[\text{HCN}]}{150} + \frac{[\text{HCl}]}{3800} + \frac{[\text{HBr}]}{3000} + \frac{[\text{NO}]}{1000} + \frac{[\text{NO}_2]}{200} \quad \text{Eq. (1)}$$

119 But this equation was not sufficient to consider the effect of CO<sub>2</sub> concentration on fire toxicity.  
 120 Therefore, FED calculations were updated (see Eq. 2) by including CO<sub>2</sub> concentration; and the  
 121 slope (m) and intercept (b) of plotting the curve of [CO] against [CO<sub>2</sub>] to describe the growing  
 122 up of CO toxicity as the [CO<sub>2</sub>] increases. In addition, O<sub>2</sub> concentration was included in this  
 123 update (ISO 13344:2015).

$$124 \quad \text{FED} = \frac{m[\text{CO}]}{[\text{CO}_2] - b} + \frac{21 - [\text{O}_2]}{(21 - 5.4)} + \frac{[\text{HCN}]}{150} + \frac{[\text{HCl}]}{3700} + \frac{[\text{HBr}]}{3000} \quad \text{Eq. (2)}$$

125 Besides Eq. (1,2), Purser model in Eq. (3) was applied also to calculate FED where the  
 126 concentration of each toxic gas was divided by its lethal concentration and multiply the result  
 127 by V<sub>CO<sub>2</sub></sub>. Where, V<sub>CO<sub>2</sub></sub> is a multiplication factor for CO<sub>2</sub>-driven hyperventilation, equal to  
 128 {1 + e[(0.14 . CO<sub>2</sub>) - 1]/2} and A is an acidosis factor, equal to {[CO<sub>2</sub>] × 0.05}.

$$129 \quad \text{FED} = \left( \frac{[\text{CO}]}{\text{LC}_{50.\text{CO}}} + \frac{[\text{HCN}]}{\text{LC}_{50.\text{HCN}}} + \frac{[\text{X}]}{\text{LC}_{50.\text{X}}} + \frac{[\text{Y}]}{\text{LC}_{50.\text{Y}}} \right) \times V_{\text{CO}_2} + A + \frac{21 - [\text{O}_2]}{(21 - 5.4)} \quad \text{Eq. (3)}$$

130 When FED value is equal to 1, the mixture of the toxic gases is cable of causing death to 50%  
131 of the animals that inhaled this mixture (Stec, 2017; Chow et al.2020). The fire toxicity of  
132 materials can also be presented by lethal concentration 50 (LC<sub>50</sub>). It is defined as the  
133 concentration of fire effluent which able to cause death in 50% of test animals at a defined  
134 exposure time. LC<sub>50</sub> can be calculated based on FED value, mass loss during combustion ( $\Delta M$ )  
135 and the volume of the combustion chamber (V) following to Eq. (4) (Chow et al. 2020).

$$136 \quad LC_{50} = \frac{\Delta M}{FED \cdot V} \quad \text{Eq. (4)}$$

137 Where, M (in g) is the specific mass loss and V (in m<sup>3</sup>) is the total air volume at standard  
138 temperature and pressure.

139 The aims behind this work were to combine TA with melamine and phosphoric acid to  
140 form a new multifunction single molecule intumescent flame retardant, MTP, for cotton  
141 fabrics. In addition, comparing the efficiency of the new SMIFR with other traditional flame-  
142 retardant systems that are based on MP and TA. The thermal stability and flammability  
143 properties of the different samples were studied by TGA, UL94, LOI, single flame source and  
144 smoke box chamber. The toxic gases evolved during combustion process were determined by  
145 FTIR gas analyser and fire toxicity of the samples was evaluated based on FED and LC<sub>50</sub> data.  
146 Tensile strength and antibacterial properties of the treated cotton samples were evaluated.

## 147 **2. Experimental**

### 148 *2.1. Materials*

149 Natural cotton fabrics (100%; 120 g/m<sup>2</sup>) were supplied by Texmar Company, Egypt. Tannic  
150 acid (C<sub>76</sub>H<sub>52</sub>O<sub>46</sub>) with M.W 1701.22 g/mol was obtained from S D Fine-Chem Limited, India.  
151 Poly (vinyl alcohol) with M.W 115000 g/mol and degree of polymerization 1700 – 1800 was  
152 purchased from Oxford Lab Chem, India. Melamine (99%) was purchased from Alfa Aesar  
153 Company, Germany. Phosphoric acid (85%) and methanol (99%) were supplied by Sigma-  
154 Aldrich Company, Germany. The chemicals were used without further purification. De ionized  
155 water was collected from deionized water unit supplied by purite select fusion unit, UK.

### 156 *2.2. Synthesis of MTP*

157 MTP was synthesized by adding 50 g phosphoric acid to 20 g TA to form tannic phosphate  
158 (TP) as intermediate. The reactants were stirred on a hot plate with stirrer at 100 °C and the  
159 reaction continued for 1 h till brown solution was obtained. In a round bottom flask with  
160 condenser, 30 g of melamine powder was dispersed in 500 mL of methanol. TP solution was  
161 added dropwise to melamine (dispersed in methanol) within 30 min, the hotplate temperature

162 was remained at 120 °C and the reaction continued for 6 h. The product (MTP) was filtered,  
163 washed with methanol, dried at room temperature for 72 h and grinded to fine powder.

164 [Fig. 1\(A\)](#) shows the synthetic route of MTP.



168

169 **Fig. 1. (A)** Schematic illustration of a suggested synthetic route of MTP; (B) the structure of  
170 cotton fabric/PVA/MTP prepared by dip-pad-dry method.

171

### 172 2.3. Preparation of MP

173 MP was synthesized according to the procedure in [Abdelkhalik et al. \(2019\)](#). In a round bottom  
174 flask linked to condenser, 30 g of melamine was scattered in 250 mL methanol and agitated for  
175 30 min at room temperature using hot plate with stirrer. Then, phosphoric acid (25 g) was  
176 added to melamine, the hot plate temperature was regulated at 120 °C and the reaction was  
177 kept for 3 h. Finally, MP was obtained, filtered, washed with 500 mL methanol to remove the  
178 excess of phosphoric acid and dried for 72 h at room temperature.

179

### 180 2.4. Preparation of flame retardant cotton fabrics

181 Cotton fabric samples were washed using deionized water and were dried at 60 °C for 1 h  
182 before using. Then, the weights of cotton samples with appropriate size were measured and  
183 recorded. A beaker containing deionized water and PVA was heated to 150 °C for 30 min  
184 using a hot plate with mechanical stirrer at 650 rpm until PVA was dissolved in deionized  
185 water. Then, MTP was added into the PVA solution with continuous stirring at 70 °C.  
186 PVA/MTP finishing solutions with different MTP concentrations (10%MTP, 20%MTP and  
187 30%MTP) were prepared. The cotton fabric samples were soaked in these solutions at 70 °C  
188 for 10 min and 90% pick-up was obtained within three pads. Then, the coated samples were  
189 dried at 100 °C for 5 min and cured at 160 °C for 3 min. The other samples which were coated  
190 with PVA/MP, PVA/TA and PVA/MP/TA were prepared according to the previous method.  
191 For durability study, the coated cotton samples were rinsed several times with tap water, dried  
192 at 70 °C for 1 h and weighed. [Fig. 1\(B\)](#) shows the structure of cotton fabric/PVA/MTP  
193 prepared by dip-pad-dry method. The weight gain (WG) of MTP-coated cotton fabrics were  
194 calculated on the basis of the equation  $WG\% = (W_a - W_b) / W_b \times 100\%$ , where,  $W_a$  and  $W_b$  are the  
195 weight of control cotton and MTP coated cotton fabrics, respectively. [Table 1](#) presents the  
196 coating composition of cotton fabric samples.

197

### 198 2.5. Characterization and measurements

199 FTIR spectra were recorded by Nicolet 380 spectrophotometer in the optical range of 4000  
200 – 400  $\text{cm}^{-1}$ . Thermogravimetric analysis (TGA) was executed by Shimadzu TGA50 under

201 nitrogen atmosphere with a flow rate 30 mL/min. TGA measurements were started from  
202 ambient temperature to 750 °C, the heating rate was 10 °C/min and the samples weights were  
203 approximately 6 – 7 mg. Vertical and horizontal flammability tests were performed using  
204 UL94 flame chamber (purchased from FTT – company, UK). The vertical test was carried out  
205 according to [ASTM D 6413:\(2015\)](#) where samples with dimensions 250 mm × 90 mm were  
206 subjected to vertical flame with 38 mm height for 12 s. The horizontal burning rate of the  
207 samples was evaluated according to [ISO 3795:\(1989\)](#) where samples were exposed  
208 horizontally to flame with 38 mm height for 15 s. The ignitability of specimens was determined  
209 by single flame source apparatus (manufactured by FTT- Company, UK). In this test a small  
210 flame with 20 mm height was directly impinged with a vertically oriented test specimen for  
211 30 s according to [ISO 11925-2:\(2020\)](#). LOI values were determined by oxygen index (supplied  
212 by Reohmetric Scientific Ltd, UK) according to standard test method [ISO 4589-2:\(2017\)](#). The  
213 samples dimensions were 120 mm length and 50 mm width. Specific optical density was  
214 determined by the smoke box chamber (manufactured by FTT - Company, UK) according to  
215 standard test method [ISO 5659-2:\(2017\)](#). The specimens' dimensions were 75 mm × 75 mm.  
216 Each specimen was wrapped in aluminium foil and subjected horizontally to external heat flux  
217 25 kW/m<sup>2</sup> under non flaming conditions. The smoke box chamber was linked to FTIR gas  
218 analyser (supplied by FTT Company, UK) to measure continuously, during smoke density test,  
219 the concentrations of the following gases: CO, CO<sub>2</sub>, H<sub>2</sub>O, NO, NO<sub>2</sub>, HCN, NH<sub>3</sub>, HCHO, C<sub>3</sub>H<sub>8</sub>,  
220 C<sub>2</sub>H<sub>6</sub> and C<sub>6</sub>H<sub>14</sub>. The concentration of O<sub>2</sub> was measured by Testo gas analyser. The recorded  
221 concentrations for gases are the average of three tested samples results. SEM images were  
222 collected by Quanta 250 FEG (Field Emission Gun) produced by FEI Company, the  
223 Netherlands. The assessment of bacteriostatic activity against Gram-positive, *Staphylococcus*  
224 *aureus* (*S. aureus*) and Gram-negative, *Escherichia coli*, (*E-Coli*) bacteria was assessed using  
225 agar diffusion test according to AATCC test method 147-2004 (Parallel Steak Method) and  
226 expressed as zone inhibition (mm). Fresh inoculants for antibacterial assessment were prepared  
227 on nutrient at 37 °C for 24 h. Any prominent zone of inhibition around the samples was  
228 recorded as an inhibitory effect against the above mentioned bacterial species. Tensile strength  
229 was measured in the strip method by using universal testing machine (Tinlus Olsen, model  
230 H5KT) according to [ISO 13934-1:\(2013\)](#).

231

232

233

234 **Table 1**

235 Coating formulations for cotton fabric samples.

Sample code	Coating composition			
	PVA %	TA %	MP %	MTP %
C0 (control sample)	0	0	0	0
C1	10	0	0	0
C2	10	10	0	0
C3	10	0	10	0
C4	10	5	5	0
C5	10	0	0	10
C6	10	0	0	20
C7	10	0	0	30
C8	10	0	0	30

236

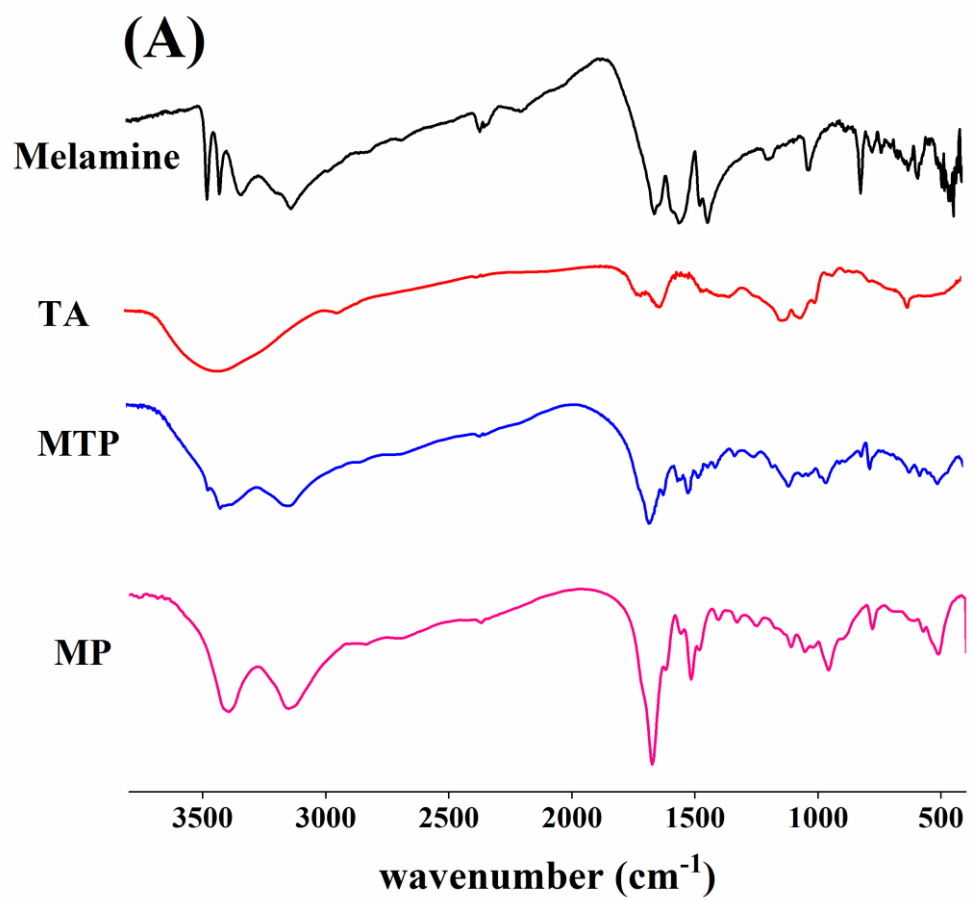
### 237 **3. Results and discussion**

#### 238 *3.1. Characterization of MP, MTP, control and coated samples*

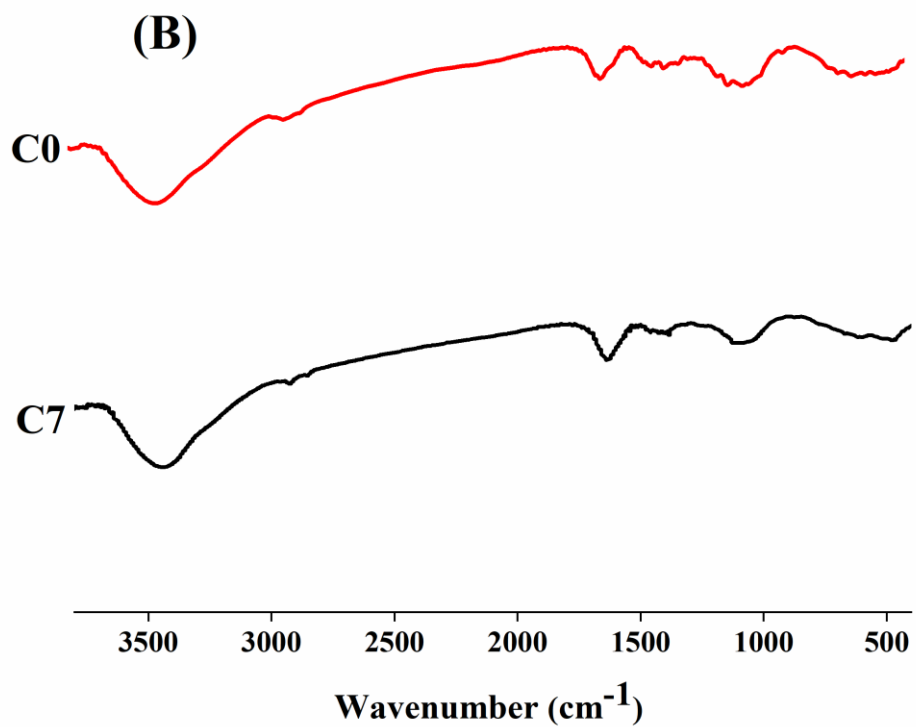
##### 239 *3.1.1 FTIR analysis of melamine, TA, MP and MTP*

240 FTIR spectra of melamine, TA, MP and MTP are presented in [Fig. 2\(A\)](#). The main absorption  
241 peaks and the corresponding functional groups are presented in [Table 2](#). The data in [Table 2](#) for  
242 melamine and TA indicates good consistency with literature data. FTIR absorption peaks of  
243 MP agree well with the data recorded in [Abdelkhalik et al. \(2019\)](#) and [Chen and Wang, \(2007\)](#).  
244 When comparing FTIR spectra of TA and MTP in [Fig. 2\(A\)](#), it can be seen formation of new  
245 peaks in MTP spectrum at  $3420\text{ cm}^{-1}$  and  $3470\text{ cm}^{-1}$  (for  $\text{NH}_2$ );  $3140\text{ cm}^{-1}$  and  $1406\text{ cm}^{-1}$  (for  
246  $^+\text{NH}_3$ );  $3370\text{ cm}^{-1}$  (for hydrogen bonded to OH);  $2680\text{ cm}^{-1}$  (for OH of  $\text{O}=\text{P}-\text{O}-\text{H}$ );  $1670\text{ cm}^{-1}$ ,  
247  $1560\text{ cm}^{-1}$  and  $817\text{ cm}^{-1}$  (for triazine ring);  $1250\text{ cm}^{-1}$ ,  $1170\text{ cm}^{-1}$  and  $1110\text{ cm}^{-1}$  (for  $\text{P}=\text{O}$ ,  $\text{P}-\text{O}$   
248 and  $\text{P}-\text{O}-\text{C}$ );  $499\text{ cm}^{-1}$  and  $619\text{ cm}^{-1}$  (for  $\text{O}-\text{P}-\text{O}$  stretching). In addition, the absorption peaks of  
249 TA at  $1620\text{ cm}^{-1}$  and  $1425\text{ cm}^{-1}$  (for  $\text{C}-\text{C}$  aromatic);  $780\text{ cm}^{-1}$  (for  $\text{C}-\text{H}$  aromatic);  $2360\text{ cm}^{-1}$

250 (for O-C=O); 1710  $\text{cm}^{-1}$  (for C=O) are also found. These data confirm the interaction between  
251 phosphoric acid, TA and melamine to form MTP.



252



253

254 **Fig. 2.** (A) FTIR spectra of melamine, MP, TA and MTP; (B) FTIR spectra of C0 and C7.

255

256

257

258

259

260

261

262

263

264

265

266

267

268

269

270 **Table 2**

271 FTIR absorption peaks of melamine, TA, MP and MTP.

Compound	Wavenumber (cm <sup>-1</sup> )	Functional group	Reference		
Melamine	3469, 3419, 3329, 3128	(-NH <sub>2</sub> ) primary amine	Makhlouf et al. (2017a,b)		
	1652, 1551, 813	Triazine ring			
TA	1028	(C-N) of primary amine	Wahyono et al. (2019); Viswanath et al. (2015)		
	3307	OH			
	2833	C-H alkane			
	2860-2920	-C-H- stretching vibrations of CH <sub>2</sub> and CH <sub>3</sub> groups			
	2360	O-C=O			
	1700	C=O			
	1205	C-O			
	1600, 1445	C – C aromatic			
	754	C – H aromatic			
	MP	3399		P-O-H, NH <sub>2</sub>	Abdelkhalik et al. (2019, 2020); Chen and Wang, (2007)
3147, 1406		<sup>+</sup> NH <sub>3</sub>			
1670		Triazine ring			
1050 ,960		P-O			
1111		P-O-H			
1254		P=O			
2680		OH in O=P-O-H			
MTP		3470, 3420	-NH <sub>2</sub>	Makhlouf et al. (2017a,b); Abdelkhalik et al. (2019, 2020); Wahyono et al. (2019); Viswanath et al. (2015)	
		3370	OH		
		3140, 1406	<sup>+</sup> NH <sub>3</sub>		
	2930 , 1320	-C-H- stretching vibrations of CH <sub>2</sub> and CH <sub>3</sub> groups			
	2840	C-H alkane			
	2680	OH in O=P-O-H			
	2360	O-C=O			
	1710	C=O			
	1620 , 1450	C – C aromatic			
	1670,1560, 820	Triazine ring			
	1410	C-N			
	1250 , 1170, 1110	P=O, P – O , P – O – C			
	780	C – H aromatic			
	617 , 499	O-P-O stretching			

272

273

274

275

276

277 3.1.2. FTIR analysis of control and coated samples

278 FTIR spectra of C0 and C7 samples are presented in Fig.2(B). It is clearly seen in FTIR  
279 spectrum of C0 absorption peaks at  $3443\text{ cm}^{-1}$  (for H bonded OH groups),  $2800 - 3000\text{ cm}^{-1}$   
280 (for C-H stretching),  $2920\text{ cm}^{-1}$  (for  $\text{CH}_2$  of long alkyl chain),  $1630\text{ cm}^{-1}$  (for adsorbed water),  
281  $1389\text{ cm}^{-1}$  (for C-H bending),  $1120\text{ cm}^{-1}$  (for C-O-C bridge),  $1044\text{ cm}^{-1}$  (for C-O stretch) and  
282  $894\text{ cm}^{-1}$  (for out-of-phase ring stretch: C1-O-C4;  $\beta$  glucosidic bond) (Chung et al. 2004).  
283 FTIR spectrum of C7 shows nearly the same absorption peaks as C0. However, there are some  
284 differences where the intensity of the peak  $1630\text{ cm}^{-1}$  increased which attributed to the  
285 presence of triazine ring in MTP. The peaks at  $1160\text{ cm}^{-1}$ ,  $1120\text{ cm}^{-1}$  and  $1044\text{ cm}^{-1}$  are merged  
286 in one broad peak in the range  $1000\text{ cm}^{-1} - 1174\text{ cm}^{-1}$ . Moreover, a new peak appeared at  $466$   
287  $\text{cm}^{-1}$  which refers to O-P-O groups (Dayanand et al. 1996).

288

289 3.1.3. SEM images of control and coated samples

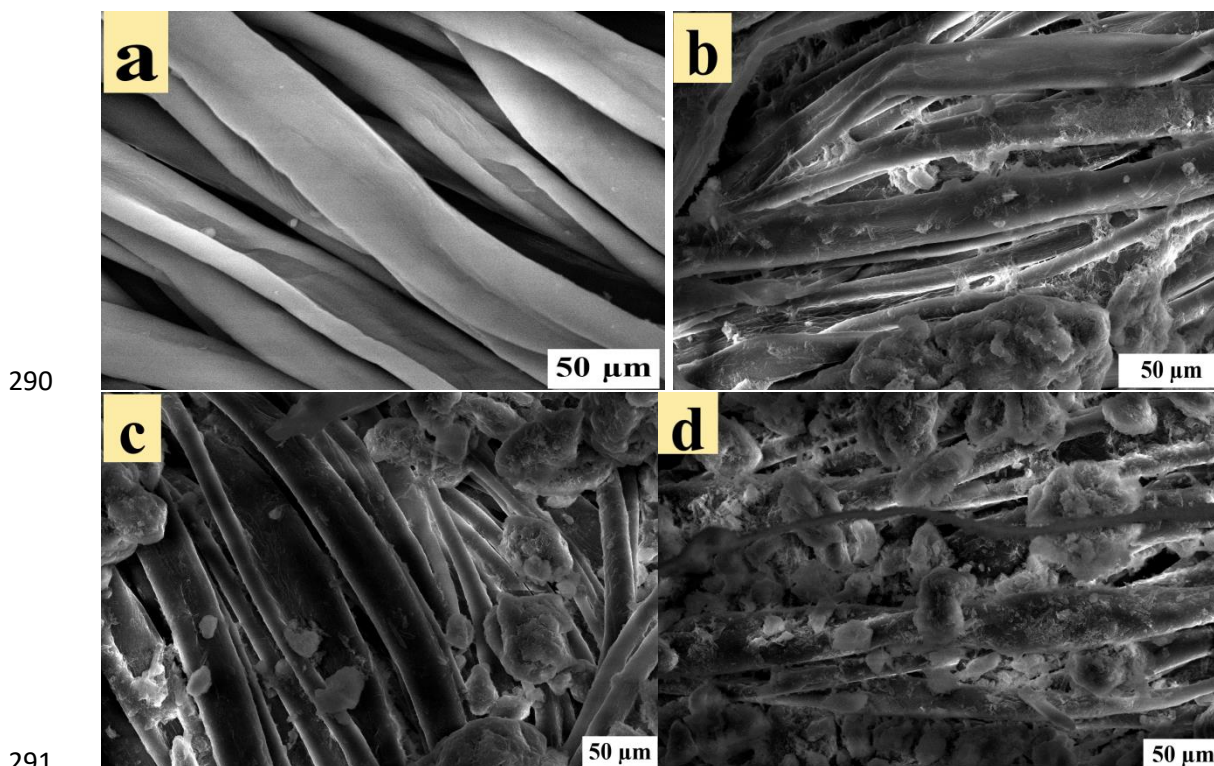


**Fig. 3.** (a-d) The surface morphology of C0, C5, C7 and C8, respectively.

293 Fig.3(a-d) shows the surface morphology of control sample and the treated samples (C5, C7  
294 and C8). The surface of control sample is smooth and clear as there is no coating on it (see Fig.  
295 3a). SEM images of treated samples show the presence of flame retardant coating on the  
296 surface and the samples are thicker than the control sample. Fig. 3(b,c) shows that the coating  
297 particles were able to penetrate into the interior of cotton fibre of C5 and C7 samples. Fig. 3(d)

299 presents that intensive particles of MTP are found on the surface of C8 sample where the  
300 sample is coated with MTP only.

301

### 302 3.2. Flammability properties

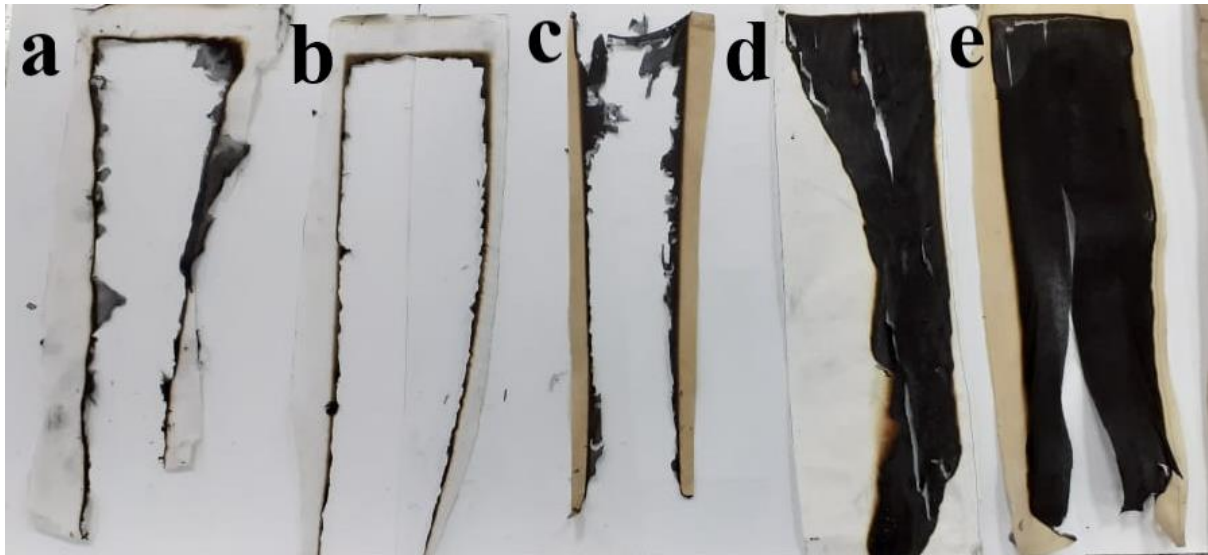
303

#### 304 3.2.1. Vertical and horizontal flammability tests

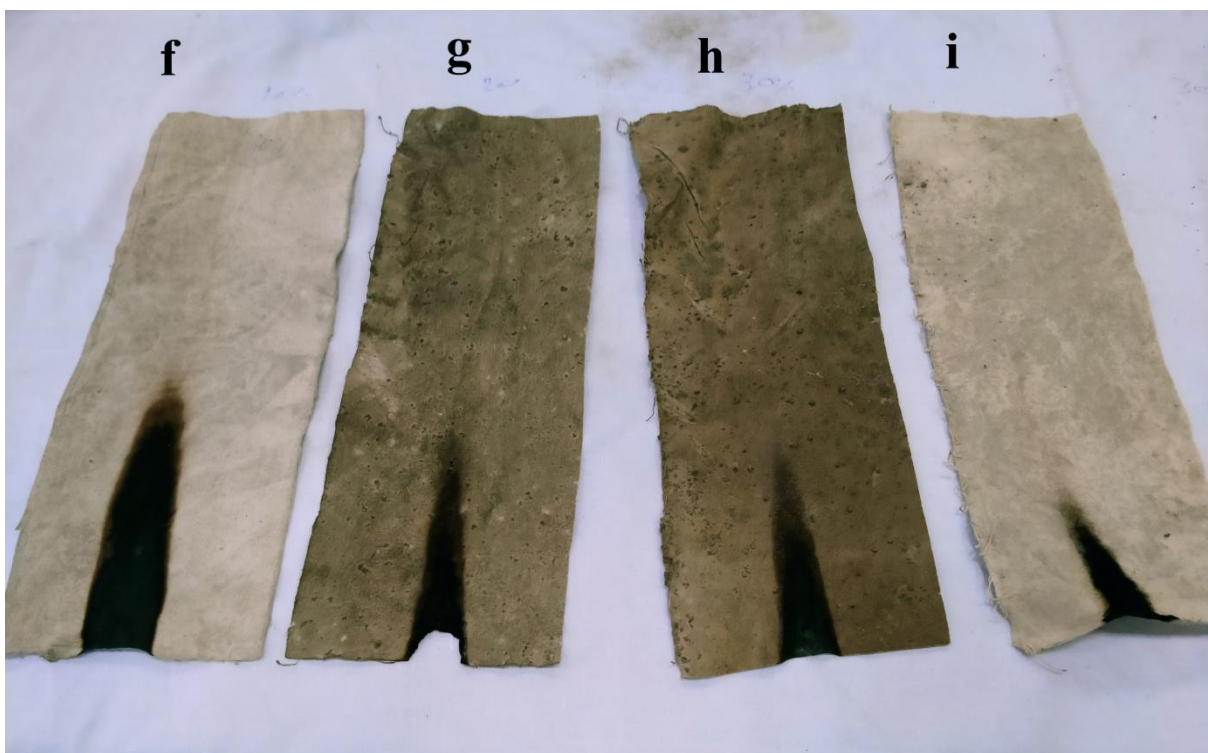
305 The data in [Table 3](#) shows the results of horizontal and vertical burning tests. In horizontal  
306 burning rate test, the control sample burnt completely and its rate of burning was 214 mm/min.  
307 In vertical flammability test, control sample burnt completely where after flame time ( $t_{af}$ ) and  
308 afterglow time ( $t_{ag}$ ) were 9 s and 36 s, respectively; and there was no residual char after the  
309 test. Addition of PVA to cotton fabric, C1 sample, did not show significant change in  
310 horizontal and vertical flammability properties of control sample (see [Table 3](#)). C2 sample data  
311 indicated that PVA/TA system reduced the rate of burning of control sample by 26.6% and  
312 increased its  $t_{af}$  to 19 s. C3 sample showed that (PVA/MP) decreased the rate of burning of  
313 control sample by 35.5%, while  $t_{af}$  raised to 30 s,  $t_{ag}$  increased to 40 s and the char length was  
314 250 mm. According to the data in [Table 3](#), C4 failed to achieve better or even the same  
315 flammability results of C3. This indicates that addition of TA to PVA/MP decreased the  
316 efficiency of PVA/MP as a flame retardant coating for cotton fabrics. The next data for LOI  
317 and smoke density for C3 and C4 showed the same behavior also. This may be referred to that  
318 MP and TA were decomposing separately at the same time and the presence of TA may be  
319 decreased the possibility of interaction between MP and PVA to form a coherent char layer on  
320 the sample surface. In contrary, C5, C6, C7 and C8 samples had burning rate 0 mm/min.  
321 Moreover,  $T_{af}$  and  $T_{ag}$  for C5, C6, C7 and C8 samples were 0 s. This confirms that PVA/MTP  
322 and MTP alone are highly efficient as flame retardants compared with PVA/TA, PVA/MP and  
323 PVA/MP/TA. [Fig. 4](#) shows the different samples after vertical flammability test. It is clearly  
324 seen in [Fig. 4\(a-c\)](#) that C0, C1 and C2 burnt completely without leaving char residue. The  
325 flame propagated to the end of samples C3 and C4 and the char length values in C3 and C4  
326 were 250 mm ([Fig. 4d,e](#)). In contrast, [Fig. 4\(f-i\)](#) shows that the flame did not propagate in  
327 samples C5, C6, C7 and C8 and the char length of these samples was 120 mm, 90 mm, 75 mm  
328 and 65 mm, respectively. It is expected that the single molecule intumescent flame retardant  
329 MTP decomposed to give CO, CO<sub>2</sub>, NH<sub>3</sub> and water vapor in the gas phase. In the condensed  
330 phase, phosphate groups decomposed to produce phosphoric acid and polyphosphoric acid  
331 which interacted with PVA, TA and cotton fabric to form coherent and compact char layer  
332 which prevented cotton from the effect of flame. In conclusion, PVA/MTP and MTP alone

333 presented high efficiency as a flame retardant for cotton fabrics in comparison with PVA/TA,  
334 PVA/MP and PVA/TA/MP. The order of different flame retardants based on their efficiency  
335 was as follow:

336 PVA/MTP and MTP > PVA/MP > PVA/MP/TA > PVA/TA > PVA.



337



338

339 **Fig. 4.** (a-i) Digital photographs for control and treated samples after vertical flammability test.

340

341

342

343

344

345 **Table 3**

346 Results of horizontal, vertical flammability and LOI tests before washing process.

Sample code	Horizontal flammability	Vertical flammability			LOI (%)
	Burning rate (mm/min)	$t_{af}$ (s)	$t_{ag}$ (s)	Char length (mm)	
C0	214	9	36	No char*	17.1
C1	211 (1.4%)	14	0	No char*	19.4
C2	157 (26.6%)	19	0	No char*	22.3
C3	138 (35.5%)	30	40	250	28.5
C4	183 (14.4%)	22	0	250	23.2
C5	0	0	0	120	39.4
C6	0	0	0	90	50.6
C7	0	0	0	75	68.4
C8	0	0	0	65	48.1

347 \*No char means that the sample burnt completely without leaving char residue.

348

349 *3.2.2. LOI data*

350 LOI is defined as the minimum concentration of oxygen, in oxygen and nitrogen mixture,  
351 which is able to support flame propagation in a vertical test sample under particular test  
352 conditions (ISO 4589-2:(2017)). The higher LOI values of samples relative to blank reflect the  
353 increase in flame retardancy of specimens. LOI data are presented in Table 3 and it shows that,  
354 in one hand, control sample had LOI value 17.1%. Addition of PVA (C1), PVA/TA (C2) and  
355 PVA/MP (C3) increased the LOI value of control sample to 19.4%, 22.3% and 28.5%,  
356 respectively. C4 sample showed LOI value 23.2%. This indicates that the coating in C4 sample  
357 (PVA/TA/MP) failed to improve LOI value compared to C3 (where PVA/MP was used as a  
358 coating). Therefore, adding TA to PVA/MP was not the best choice to improve the flame  
359 retardancy of cotton fabrics. On the other hand, C5, C6 and C7 samples showed LOI values  
360 39.4%, 50.6% and 68.4%, respectively. This means that the addition of PVA/MTP to cotton  
361 fabric enhanced greatly its flame retardancy. And as the loading level of MTP increased in the

362 coating formulation, LOI value was increased. It is clearly seen in [Table 3](#) that PVA/MTP  
363 system (C5, C6, C7) was highly efficient compared with PVA/MP system (C3). In addition, the  
364 coating of C7 was more efficient as a flame retardant than the coating of C8 sample (MTP  
365 alone) which had LOI value 48.1%. This means that PVA participated with MTP in improving  
366 the flame retardancy of control sample through fixing MTP inside cotton fabric and enhancing  
367 formation of thermally stable char layer on samples surface.

368

### 369 *3.2.3. Single flame source test*

370 The single flame source test was performed in order to subject the control and coated samples  
371 to direct flame for time more than 12 s. This test is a part of fire tests which are used to  
372 evaluate the fire performance of building materials. According to [ISO 11925-2:\(2020\)](#), the  
373 flame can be applied to sample for 30 s or 15 s. Also the flame can be applied at midpoint of  
374 bottom edge of sample or at the sample surface after 40 mm from the bottom edge. In this  
375 work, the flame was applied at the midpoint of bottom edge for 30 s and the total test duration  
376 was 60 s. The sample is considered pass the test when the flame front doesn't exceed the  
377 reference mark at 150 mm within 60 s (30 s as flame application time + 30 s after removing the  
378 ignition source away from the sample). It is clearly seen in [Table 4](#) that the samples C0, C1,  
379 C2, C3 and C4 failed to pass the test where the flame front reached the reference mark at 150  
380 mm within 60 s. In contrast, the samples C5, C6, C7 and C8 did not ignite and passed the test.  
381 This means that addition of PVA/MTP and MTP (alone) to cotton fabrics enhanced greatly its  
382 flame retardancy. Moreover, the single molecule intumescent flame retardant, MTP, in  
383 PVA/MTP system was more efficient than PVA/TA, PVA/MP and PVA/MP/TA mixtures.  
384 According to [BS EN 13501-1:\(2018\)](#), the samples C5, C6, C7 and C8 fulfil the requirements of  
385 classes B, C, D, E concerning single flame source test only. But other large scale fire tests such  
386 as single burning item test will be necessary to consider the samples achieve completely class  
387 B, C and D requirements ([BS EN 13501-1:\(2018\)](#)).

388

389

390

391

392

393

394

395

396

397 **Table 4**

398 Results of single flame source test.

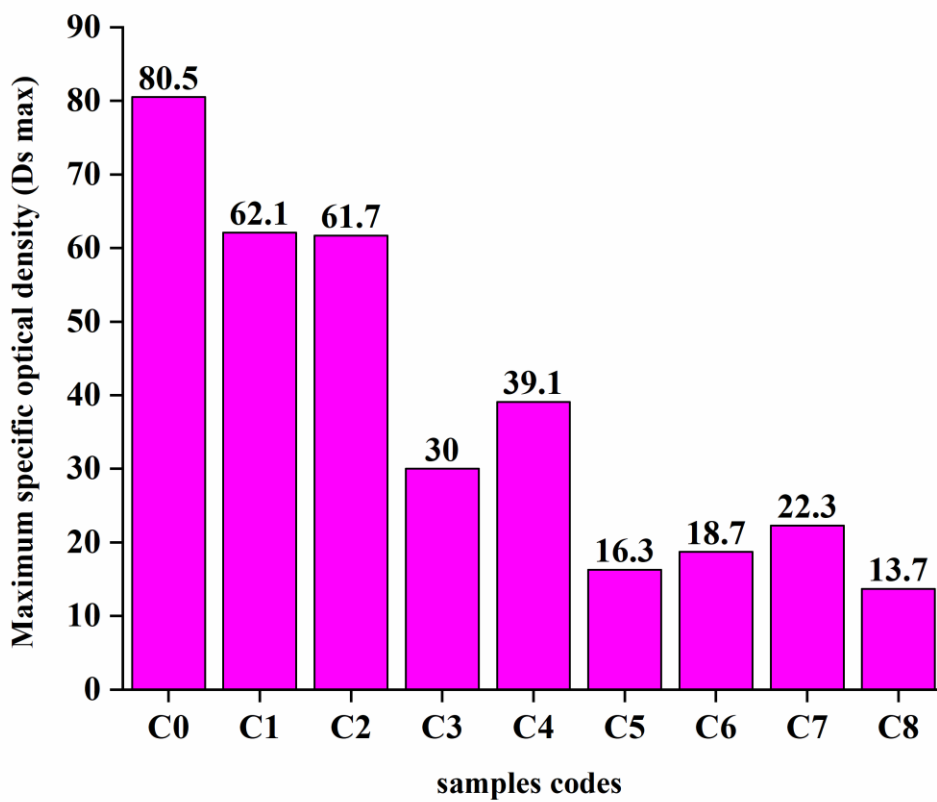
Sample code	Parameters				
	Occurrence of ignition	Whether Flame exceed 150 mm	Time to exceed 150 mm ( $t_{150}$ , s)	Ignition of filter paper	Classification
C0	Yes	Yes	35	No	F
C1	Yes	Yes	42	No	F
C2	Yes	Yes	37	No	F
C3	Yes	Yes	55	No	F
C4	Yes	Yes	51	No	F
C5	No	No	0	No	B,C,D,E
C6	No	No	0	No	B,C,D,E
C7	No	No	0	No	B,C,D,E
C8	No	No	0	No	B,C,D,E

399

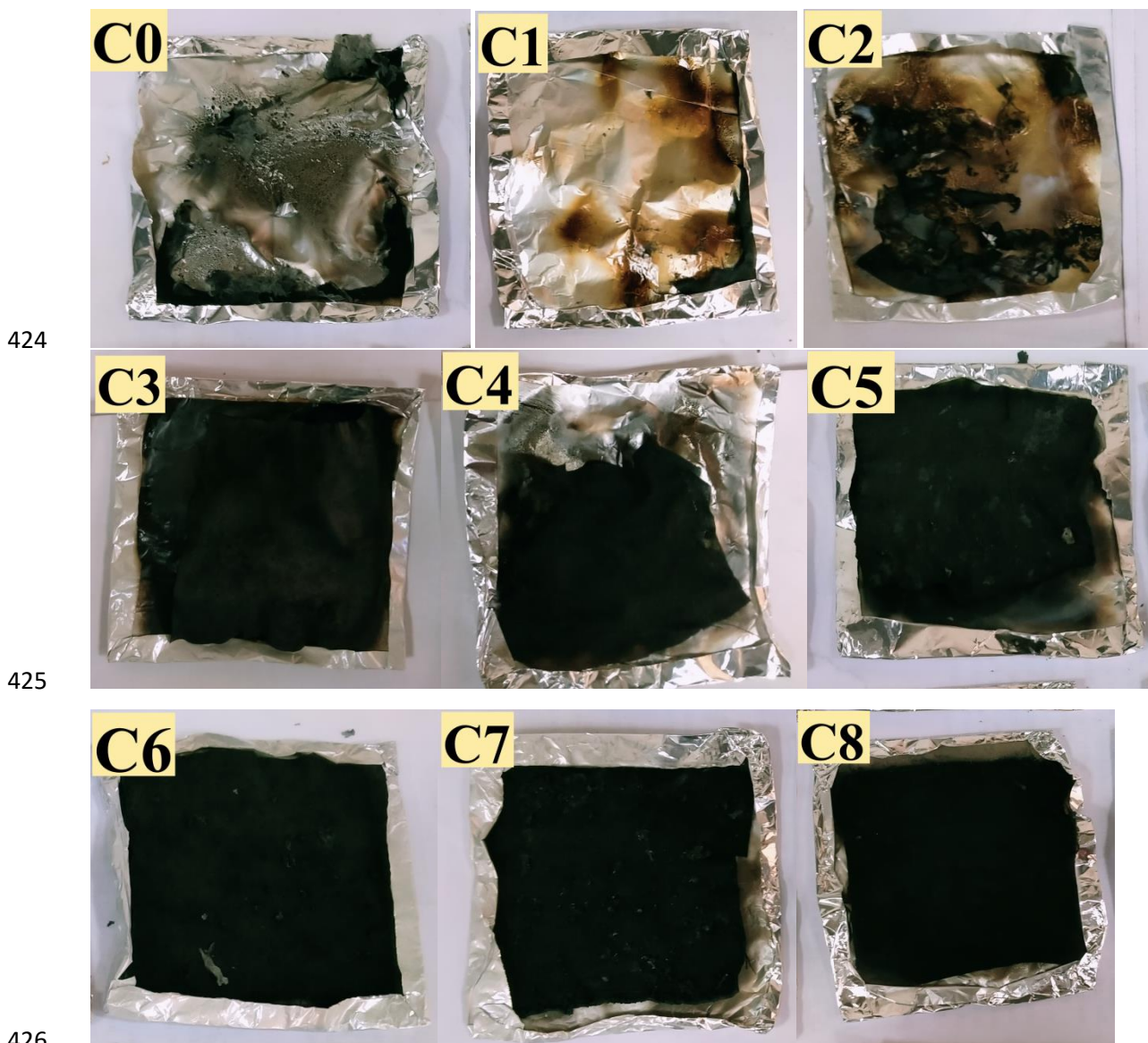
400 *3.2.4. Smoke density*

401 The data in Fig. 5 shows the maximum specific optical density ( $D_{S_{max}}$ ) for all samples at 25  
402 kW/m<sup>2</sup> and non-flaming conditions.  $D_{S_{max}}$  of control sample was 80.5 and it decreased in C1  
403 and C2 samples by 22.8% and 23.3%. PVA/MP and PVA/MP/TA minimized  $D_{S_{max}}$  of cotton  
404 fabrics by 62.7% and 51.4% as it is shown in C3 and C4 results. This indicates that PVA/MP  
405 mixture was more efficient as a smoke suppressant than PVA/MP/TA mixture. The samples  
406 C5, C6, C7 and C8 showed the maximum reductions in  $D_{S_{max}}$  and the amounts of these  
407 reductions were 79.7%, 76.7%, 72.2 and 82.9%, respectively. This is referred to formation of a  
408 protective char layer on the cotton fabric surface which saved the underlying polymer from the  
409 effect of heat. The digital photographs in Fig. 6 for the samples after smoke density test  
410 confirmed this suggestion. It is clearly seen in Fig. 6 that C0, C1 and C2 samples  
411 approximately bunt completely. The char residue of C3 sample was coherent and covered the  
412 whole sample meanwhile the char residue of C4 was discontinuous and the sample burnt

413 completely at certain parts. This confirms that PVA/MP mixture was more efficient as flame  
414 retardant than PVA/MP/TA. The char residue of samples C5, C6, C7 and C8 in Fig. 6 was  
415 continuous, coherent, and compact and were able to protect the underlying cotton samples from  
416 the effect of heat and oxygen. This led to higher reductions in  $D_{S_{max}}$  values of C5, C6, C7 and  
417 C8 relative to C0. According to smoke density data, the order of the efficiency of different  
418 additives as a smoke suppressant is  $MTP > PVA/MTP > PVA/MP > PVA/MP/TA > PVA/TA >$   
419  $PVA$ .  
420



421  
422 **Fig. 5.** Values of maximum specific optical density ( $D_{S_{max}}$ ) for control and coated samples.



427 **Fig. 6.** Digital photographs of control and treated samples after smoke density test.

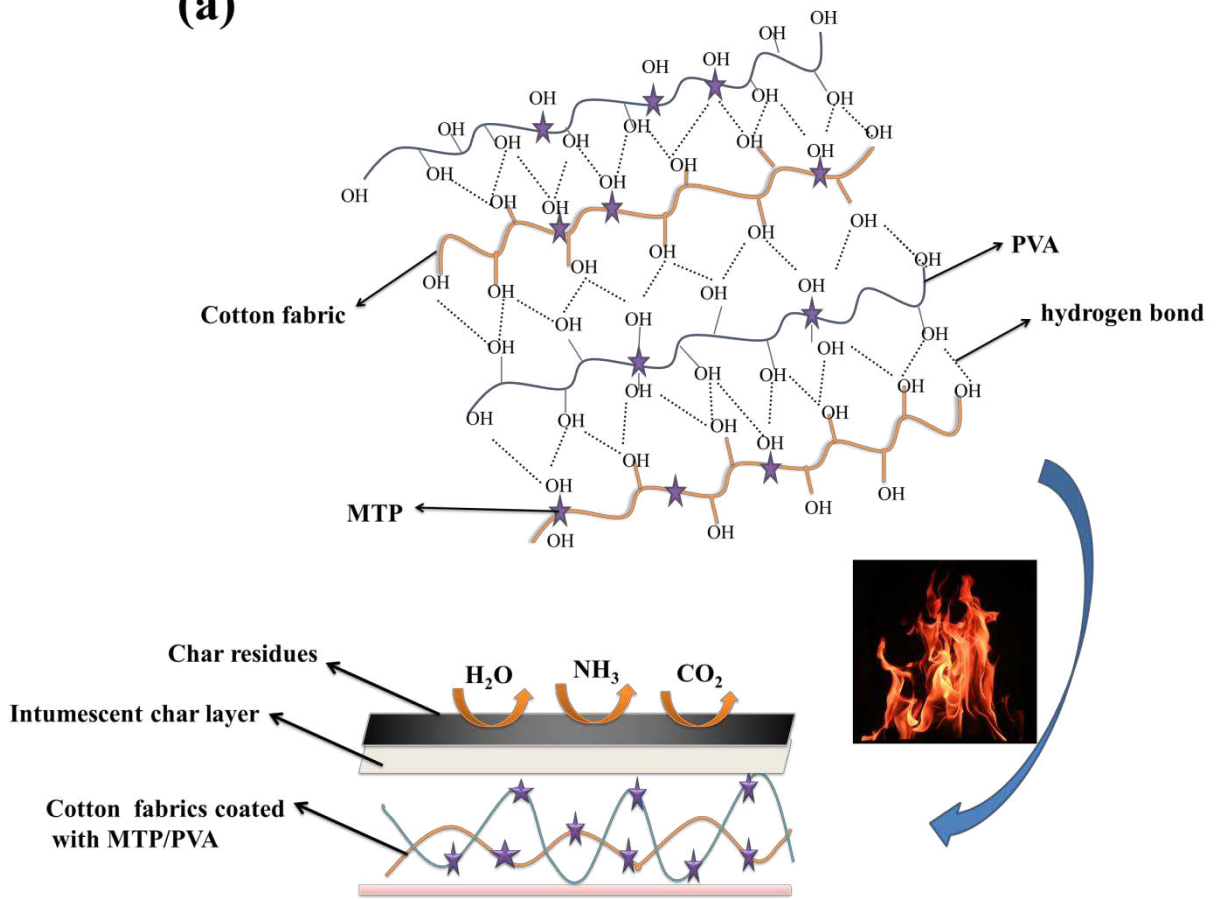
428

### 429 3.2.5 FTIR gas analyser data and flame retardant mechanism

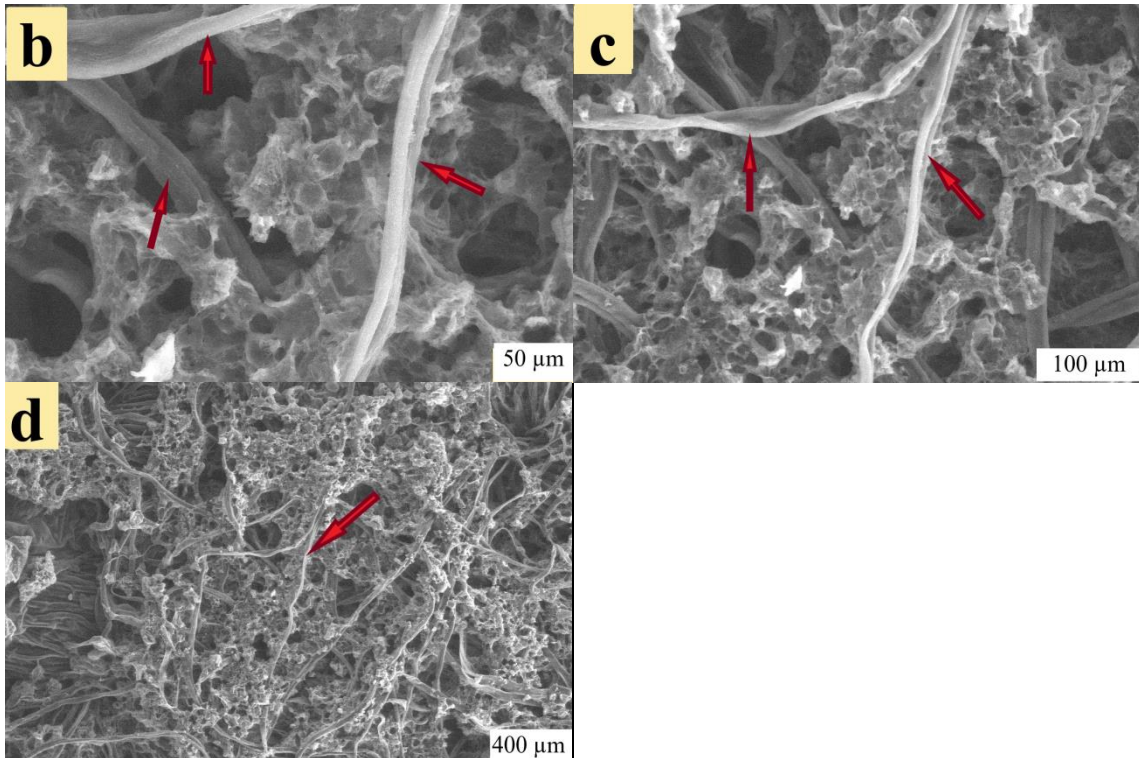
430 FTIR gas analyser connected to smoke box chamber was used to identify the combustion  
 431 products in the gas phase. The data in [Table 5](#) shows the average values for the concentrations  
 432 of gases which are detected by FTIR gas analyser. According to the data in [Table 5](#), control  
 433 sample decomposed and gave out mainly CO, CO<sub>2</sub>, water vapour, HCHO, C<sub>2</sub>H<sub>6</sub> and C<sub>6</sub>H<sub>14</sub>. In  
 434 addition, NO, HCN, CH<sub>4</sub>, C<sub>2</sub>H<sub>4</sub> and C<sub>3</sub>H<sub>8</sub> were detected at minor concentrations. The presence  
 435 of NO and HCN in combustion products of C0 sample is referred to the oxidation of nitrogen  
 436 in the air which was found inside the smoke box chamber. The addition of PVA to cotton  
 437 fabric, sample C1, increased the concentrations of water vapour, CO, C<sub>3</sub>H<sub>8</sub>, C<sub>6</sub>H<sub>14</sub> and C<sub>2</sub>H<sub>6</sub>.

438 The gases HCHO and CO<sub>2</sub> were also produced, but at lower concentrations compared to  
439 control sample. The increase in hydrocarbon gases (C<sub>3</sub>H<sub>8</sub>, C<sub>6</sub>H<sub>14</sub> and C<sub>2</sub>H<sub>6</sub>) concentrations is  
440 referred to the decomposition of PVA. It was reported that PVA decomposition takes place  
441 through dehydration, depolymerization and polyene formation. Then, pyrolysis of polyene  
442 formed and producing certain volatile organic compounds (Zaikov and Lomakin, 1998;  
443 Gaikwad et al. 2015; Dong et al. 2016). FTIR gas analyser data for C2, C3 and C4 samples  
444 showed that addition of PVA/TA, PVA/MP and PVA/MP/TA to cotton fabric succeeded in  
445 decreasing its CO and CO<sub>2</sub> production during combustion. Also, the production of hydrocarbon  
446 gases (C<sub>3</sub>H<sub>8</sub>, C<sub>6</sub>H<sub>14</sub> and C<sub>2</sub>H<sub>6</sub>) was also reduced. The maximum reductions were observed in C3  
447 sample where PVA/MP retarded the effect of heat through the formation of a coherent char  
448 layer on the cotton sample surface. But the presence of MP in the samples C3 and C4 led to  
449 increasing in the concentrations of NH<sub>3</sub> and HCN relative to control sample. This is referred to  
450 the decomposition of melamine in MP structure. The data in Table 5 manifested that C5, C6,  
451 C7 and C8 samples which contains PVA/MTP and MTP alone as coatings produced the highest  
452 concentrations of NH<sub>3</sub> and water vapour relative to the other samples. In addition, the  
453 production of CO, HCHO and hydrocarbon gases were decreased relative to C0, C1, C2, C3,  
454 and C4 samples. This indicates that degradation of MTP produced water vapour, CO<sub>2</sub> and NH<sub>3</sub>  
455 (in the gas phase) which diluted the concentrations of volatile organic compounds and oxygen  
456 in the combustion zone. Moreover, the great reduction in the concentrations of HCHO and  
457 hydrocarbon gases indicates that PVA and cotton fabrics in C5, C6, C7 and C8 samples  
458 maintained most of their main structure during combustion. This is referred to formation of  
459 coherent, continuous and compact char layer on cotton fabric, see Fig. 7(a). This char acted as  
460 a physical barrier and protected the cotton fabric from the effect heat and flame.

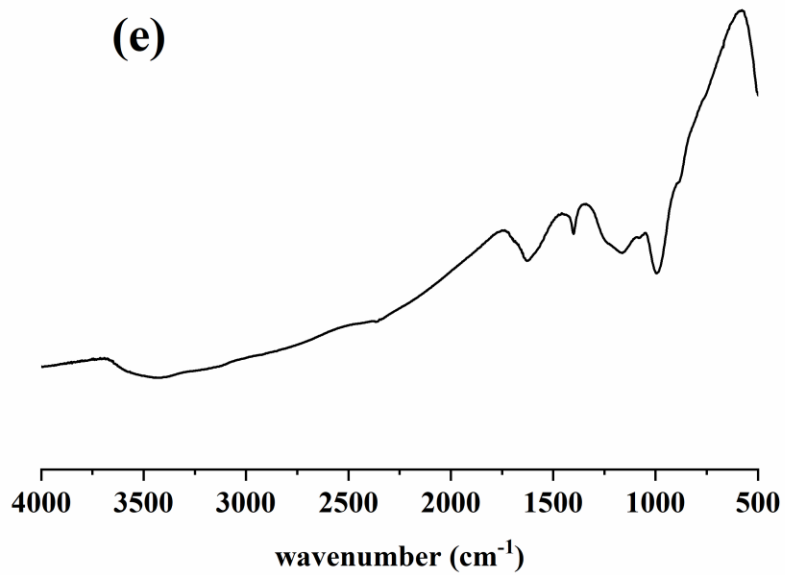
(a)



461  
462  
463



464  
465



466

467 **Fig. 7.** (a) Schematic illustration of a possible flame retardant mechanism for cotton fabrics  
468 treated with PVA/MTP during combustion; (b-d) SEM images for char residue formed after  
469 smoke density test of C7; (e) FTIR analysis of char residue of C7 after smoke density test.

470

471

472

473

474

475

476

477

478

479

480

481

482

483

484

485

486

487 **Table 5**

488 FTIR gas analyser results for control and treated samples.

Sample codes	C0	C1	C2	C3	C4	C5	C6	C7	C8
Gases									
H <sub>2</sub> O(v)	1.05	1.32	1.44	1.28	1.3	1.45	1.73	1.81	1.64
%									
CO	299	375.5	236.1	115.8	300.4	215.6	49.2	45.8	73.1
Ppm									
CO <sub>2</sub>	0.040	0.031	0.036	0.028	0.029	0.032	0.095	0.132	0.075
%									
O <sub>2</sub>	20.6	20.6	20.7	20.7	20.7	20.8	20.8	20.8	20.8
%									
HCHO	28.7	20.1	11.2	9.5	10.3	6.7	1.8	2.5	4.3
Ppm									
NO	5.9	8.6	9	9.5	10.6	10.4	11.1	10.6	10
Ppm									
NO <sub>2</sub>	7.6	2.2	1.4	1.5	1.8	3.9	7.4	8.1	5.5
Ppm									
NH <sub>3</sub>	1	1.7	2.5	29.8	11.8	22.6	75.3	110.8	130.2
Ppm									
HCN	2.1	3.4	5.7	10.6	11.2	12.9	11.4	15.2	9.7
Ppm									
C <sub>2</sub> H <sub>6</sub>	16.3	48.1	20.4	6.8	3.2	6.1	5.2	4.7	4.4
Ppm									
C <sub>3</sub> H <sub>8</sub>	8.7	29.5	15.2	2	5.6	2.8	3.6	3.6	3.3
Ppm									
C <sub>6</sub> H <sub>14</sub>	12.1	35	26.4	13.5	12.7	8.6	7.6	5.7	8
Ppm									

489

490 3.2.5.1 SEM image of char residue

491  
492 Fig. 7(b-d) shows the surface morphology of the char residue of C7 sample after the smoke  
493 density test. It is clearly seen that the fibres are grouped together, and the surface was wrapped  
494 and protected by a char layer with cellular structure. These properties are referred to that  
495 PVA/MTP coating produced during C7 combustion polyphosphoric acid which promoted the  
496 dehydration and carbonization of cotton fibre. Moreover, the degradation of PVA/MTP sent  
497 out NH<sub>3</sub>, CO<sub>2</sub> and water vapour. These gases led to char intumesce. Besides, these gases dilute  
498 volatile organic compounds and oxygen in the combustion zone. The intumescent char layer  
499 acted as a barrier and protected the cotton from the effect of heat and flame; and reduced the  
500 escaping of volatile organic compounds from the substrates to combustion zone, see Fig. 7(a).

501

502 3.2.5.2 FTIR analyses of char residue

503 The char residue after smoke density test for C7 sample was analysed by FTIR. Fig. 7(e) shows  
504 broaden peak at 2800 -3600 cm<sup>-1</sup> due interfering between the peak at 3450 cm<sup>-1</sup> which is  
505 referred to hydrogen bonded OH group and the peak at 2920 cm<sup>-1</sup> which was attributed to CH<sub>2</sub>  
506 group. This confirms the presence of carbon hydrogen chains in the char structure. The peak at  
507 1630 cm<sup>-1</sup> is for aromatic structure, the peak at 1400 cm<sup>-1</sup> is for C-N and C=N groups, the peak  
508 at 1160 cm<sup>-1</sup> is for P-O, the peak at 1050 cm<sup>-1</sup> is for P-O-C, the peak at 984cm<sup>-1</sup> is for  
509 polyphosphate and/or pyrophosphate, the peak at 881 cm<sup>-1</sup> is for alkene, the peak at 492cm<sup>-1</sup> is  
510 for O-P-O group (Abdelkhalik et al. 2020, 2019; Wahyono et al. 2019; Makhoulouf et al.  
511 2017a,b; Viswanath et al. 2015; Chen and Wang, 2007).

512 3.2.6 Smoke toxicity

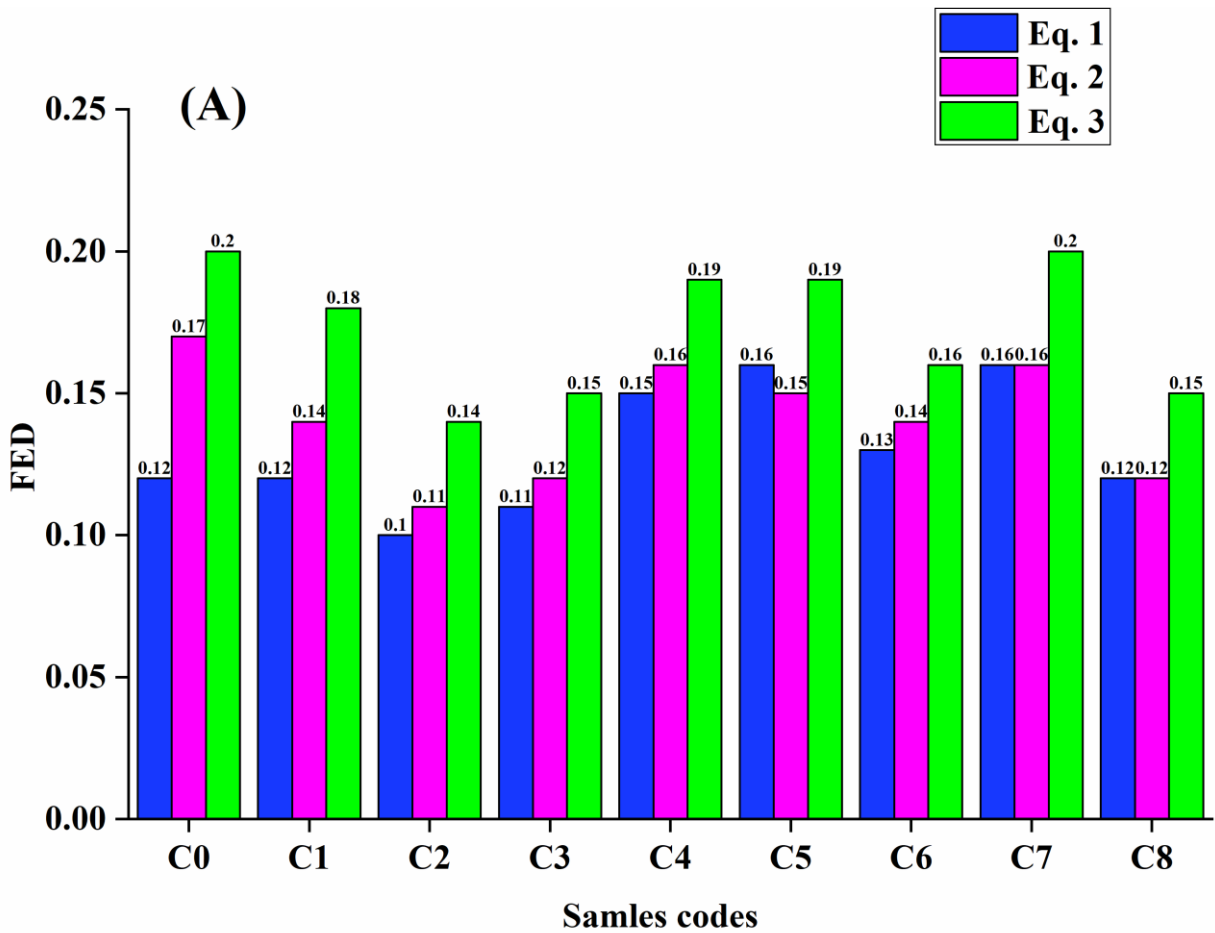
513 Fire toxicity for all samples was evaluated based on FED and LC<sub>50</sub> data. FED values were  
514 calculated using equations (1,2,3) where the following gases were taken into account: CO,  
515 CO<sub>2</sub>, NO, NO<sub>2</sub>, O<sub>2</sub>, HCN, and HCHO. Fig. 8(A) shows that FED values of control and treated  
516 samples are lower than 1 regardless the equation used in the calculation. Following to Eq. (1),  
517 the samples C4, C5, C6 and C7 have FED values greater than the control sample, but the  
518 maximum difference between blank and these samples is very low (0.04) as it is obvious in  
519 Fig. 8(A). According to Eq. (2), FED values for treated samples are lower than the control  
520 sample which means lower toxicity. Fig. 8(A) presents that calculating FED using Eq. (3) leads  
521 to lower FED values for all treated samples relative to cotton fabric. The only exception was  
522 C7 which has FED value (0.2) equal to FED value of blank. The data of Eq. (2,3) indicates that  
523 the different formulations for coating were able to decrease the fire toxicity of cotton fabrics.

524  $LC_{50}$  values were calculated according to Eq. (4) where FED values were obtained following to  
525 Eq. (3). Fig. 8(B) shows that all samples have  $LC_{50}$  value greater than the control sample. This  
526 indicates that coated samples are less toxic than the control sample. The maximum values for  
527  $LC_{50}$  were observed in C5, C6, C7 and C8 which means that PVA/MTP and MTP coatings  
528 were able to reduce fire toxicity of cotton fabrics.

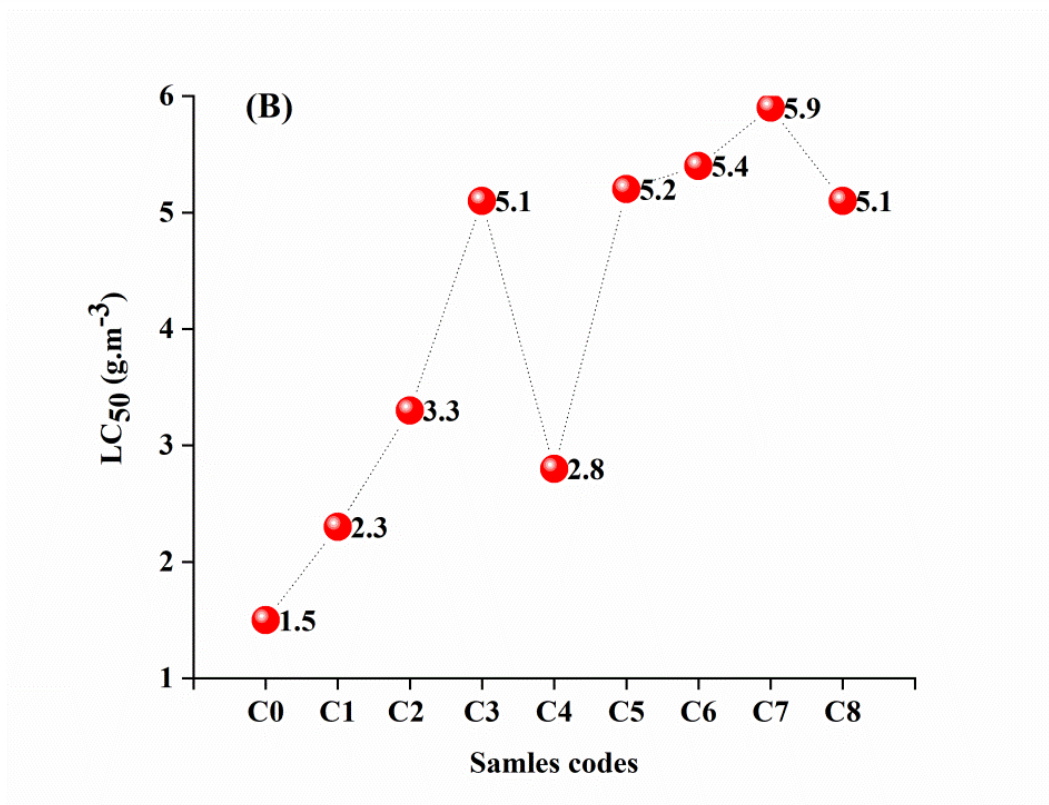
529

530

531

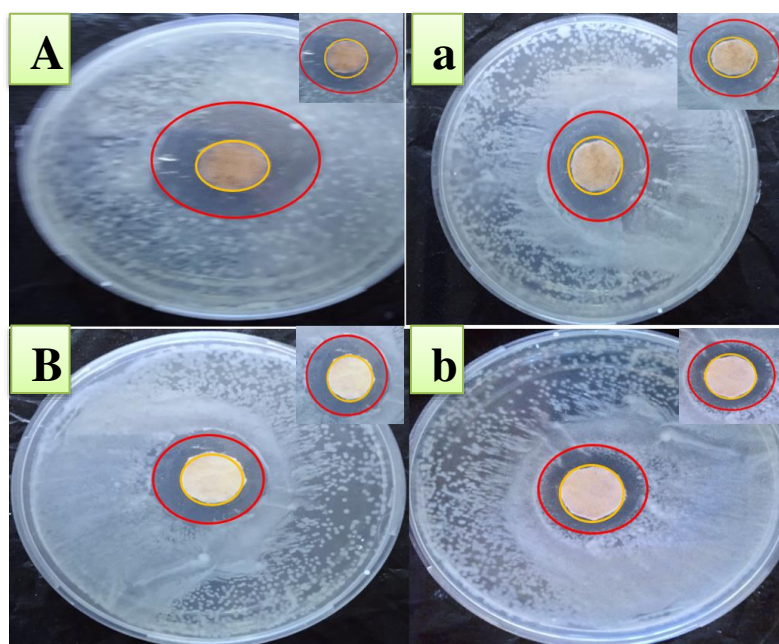


532



533

534 **Fig. 8.** (A) FED and (B) LC<sub>50</sub> values of control and treated samples.



536

537 **Fig. 9.** (A,B) digital photographs for zone of inhibition formed by *S.aureus* in C7 and C8  
 538 respectively; and (a,b) digital photographs for zone of inhibition formed by *E. coli* in C7 and  
 539 C8, respectively.

540

541 The data in [Table 6](#) show antimicrobial activity inhibition zone in (mm) for C0, C5, C6, C7 and  
 542 C8. The results prove that there is no zone of inhibition (ZOI) on uncoated cotton (C0),  
 543 indicating that it has no antibacterial property. However, the antibacterial activity was  
 544 enhanced when the concentration of MTP increased in the coating formulation. This may be  
 545 referred to the amine groups in MTP, which are in the form of  $^+NH_3$  and have positive charges,  
 546 interacted with the negative charges on the surface of bacteria cells. This interaction led to  
 547 expanded changes in the cell surface and cell permeability and causes a leakage of thiol of  
 548 protein. [Fig. 9\(A,a,B,b\)](#) displays the effect of G+ve and G-ve bacteria on the sample treated by  
 549 MTP in the absence as well as presence of PVA. It is clearly seen that the bacteria die on the  
 550 surface of coated fabric and inhibition of the growth of bacteria around the coated fabric.

551 According to the data in [Table 6](#), inhibition of *S. aureus* is more dominant than *E-coli*. This is  
 552 attributed to the mode of action of MTP on bacteria includes binding of the cationic MTP with  
 553 anionic cell surface. The results of antibacterial properties indicated that MTP can be used in  
 554 home and antimicrobial textile.

555

556

557 3.2.8 Mechanical properties

558 The data in Table 6 shows tensile strength of control and treated samples. It can be seen that  
559 the tensile strength value of control sample decreases with the addition of PVA/MTP and MTP  
560 alone. In addition, as the loading level of MTP increases, in PVA/MTP system, the tensile  
561 strength value decreases relative to blank. The reductions in tensile strength are 6.5%, 9.1%,  
562 18.1% and 3.6% in C5, C6, C7 and C8, respectively which means that PVA/MTP and MTP  
563 coatings have a slight negative effect on the tensile strength.

564

565 **Table 6**

566 Tensile strength and antimicrobial activity of control and treated samples.

Sample code	Tensile strength (N)	Antimicrobial activity (Inhibition zone in mm)	
		S.aureus G+ve	E.coli G-ve
C0	320.4	0	0
C5	299.5	12.2	10.6
C6	291.2	15.3	10.4
C7	262.4	22.5	17.6
C8	308.8	20.2	16.4

567

568

569

570

571

572

573

574

575

576 3.2.9 TGA of control and treated samples

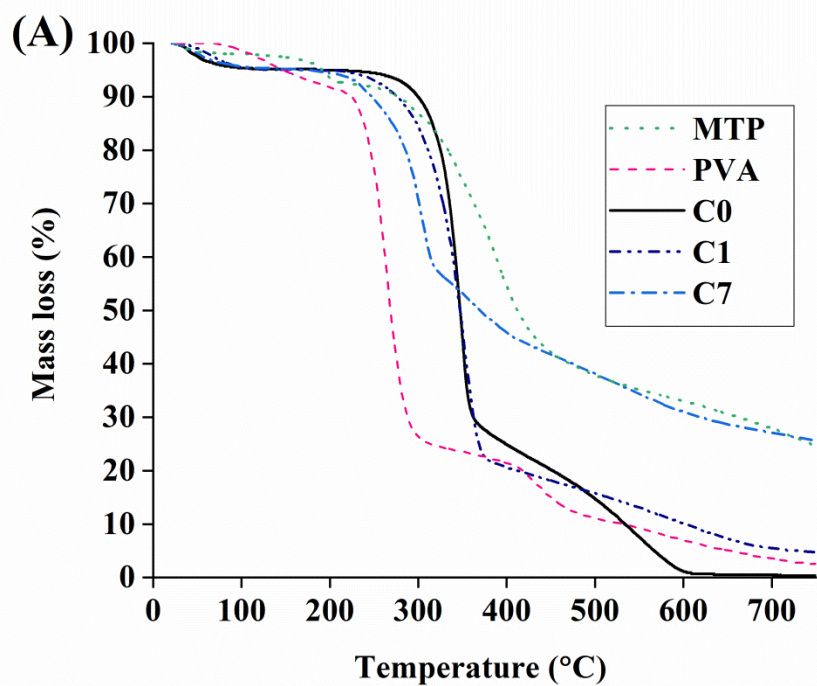
577

578 **Table 7**

579 TGA data of MTP, PVA, C0, C1 and C7, respectively.

Sample code	$T_{10\%}$ °C	$T_{50\%}$ °C	$T_{\max}$ °C	Max. mass loss mg/min	Char at 750 °C Wt.%
MTP	285	414	390	0.29	24.6
PVA	224	269	266	0.89	2.5
C0	300	347	348	1.19	0.3
C1	276	346	351	0.9	4.4
C7	251	371	304	0.5	25.5

580



581

582



583

584 **Fig. 10.** (A) TGA curves of MTP, PVA, C0, C1 and C7; (B) Digital photographs of C7, C6 and  
 585 C5 samples after washing and performing vertical flammability test.

586

587

588 TGA was used to study the thermal degradation of MTP, PVA, C0, C1 and C7 samples. The  
589 data for thermal analysis are presented in [Table 7](#) and [Fig. 10\(A\)](#). MTP shows, in [Fig. 10\(A\)](#),  
590 two decomposition steps. The first degradation step locates between 25 °C and 205 °C and  
591 includes 5.6% weight loss which is signed to losing moisture. The second decomposition step  
592 is between 208 °C - 493 °C and it involves 54.2% weight loss. During this step,  $T_{50\%}$  (at 414  
593 °C) and  $T_{\max}$  (at 390 °C) are attained. This step includes dehydration of OH group and  
594 abstracting NH<sub>2</sub> group to form non-flammable gases besides evolving of CO and CO<sub>2</sub>. In  
595 addition, phosphate ester groups decomposed to form polyphosphoric acid which interacted  
596 with other elements (C, O, N) to form carbonous char layer. The gradual growing up in  
597 temperature after 493 °C leads to a gradual increase in weight loss and the residual char at  
598 750 °C is 24.6%. PVA sample reaches  $T_{10\%}$ ,  $T_{50\%}$  and  $T_{\max}$  at 224 °C, 269 °C and 266 °C,  
599 respectively, and it leaves 2.5% as char residue at 750 °C. The thermal degradation of PVA  
600 takes place through two steps where the first stage includes dehydration and depolymerization  
601 of PVA; and polyene formation. The second decomposition step involves pyrolysis of polyene  
602 and it is accompanied by producing certain volatile organic compounds ([Zaikov and Lomakin,  
603 1998](#); [Gaikwad et al. 2015](#); [Dong et al. 2016](#)). C0 sample attains  $T_{10\%}$ ,  $T_{50\%}$  and  $T_{\max}$  at 300 °C,  
604 347 °C and 348 °C, respectively. The main decomposition stage of cotton sample locates  
605 between 280°C - 400 °C and it is accompanied with 68.5% weight loss. Thermal degradation of  
606 C0 sample takes place either through depolymerization from sugar-based units to form volatile  
607 compounds (chiefly including levoglucosan, furan, and furan derivatives) or by glycosyl unit  
608 dehydration to form aromatic char layer which is thermally stable compound ([Carosio et al.  
609 2015](#); [Wan et al. 2020](#)). Coating cotton fabric with PVA alone decreased its  $T_{10\%}$  and  $T_{50\%}$  by  
610 24 °C and 1 °C, respectively; and increased  $T_{\max}$  by 3 °C. The reduction in  $T_{10\%}$  of C1 relative  
611 to C0 is referred to dehydration and depolymerization of PVA layer on the cotton fabric  
612 surface. TGA data of C7 show that it attains  $T_{10\%}$  at 251 °C. This great reduction in  $T_{10\%}$   
613 relative to C0 is attributed to the earlier degradation of PVA/MTP coating which accompanied  
614 by evolving of water vapour, ammonia and other volatile compounds.  $T_{50\%}$  of C7 is increased  
615 by 24 °C relative to C0 and by 25 °C relative C1.  $T_{\max}$  of C7 was attained at lower temperature  
616 (304 °C) compared with C1 and C7. This may be referred to decomposition of MTP to form  
617 polyphosphoric acid which can accelerate decomposition and interaction with O and C atoms  
618 to form an insulating char layer containing polyaromatic structure. The maximum weight loss  
619 rate was 1.19 mg/min in C0 and it decreased to 0.5 mg/min in C7. Moreover, the char residue  
620 at 750 °C increased from 0.3% and 4.4% in C0 and C1 to 25.5% in C7. This indicated that  
621 MTP assisted in the formation of an insulating char layer which protected cotton fabric from

622 the effect of heat, oxygen and slow down the degradation process of C7 sample. Moreover,  
 623 emission of gases such as NH<sub>3</sub>, CO<sub>2</sub> and water vapour expelled degradation heat and decreased  
 624 the temperature of the treated cotton sample surface (Levchik et al. 1996; Xu et al. 2019; Wan  
 625 et al. 2020).

626

627 *3.2.10 Durability study*

628

629

630 **Table 8**

631 Results of horizontal, vertical flammability and LOI tests after washing process.

Sample code	Horizontal flammability	Vertical flammability			LOI (%)
	Burning rate (mm/min)	$t_{af}$ (s)	$t_{ag}$ (s)	Char length (mm)	
C5	65	7	0	250	24.2
C6	0	0	0	110	33.5
C7	0	0	0	90	49.8
C8	206.1	0	0	No char*	18.5

632 \*No char means that the sample burnt completely without leaving char residue.

633

634

635 The flammability properties of coated samples were studied after washing samples using tap  
 636 water and drying them at 60 °C for 60 min. The results of horizontal and vertical flammability  
 637 tests after washing are presented in Table 8. In horizontal flammability test, the flame  
 638 propagated in samples C5 and C8 and the rate of burning was 65 mm/min and 206.1 mm/min.  
 639 Meanwhile, flame failed to spread in C6 and C7 and the burning rate was 0 mm/min. In vertical  
 640 flammability test, C5 results manifested that the flame attained the far end of the sample (char  
 641 length 250 mm) and  $T_{af}$  was 7 s. The flame propagation was decreasing as the concentration of  
 642 MTP in PVA/MTP coating increased. C6 and C7 showed char length values 110 mm and 90  
 643 mm; and  $T_{af}$  results were 0 s which meant that C6 and C7 coatings still have high flame  
 644 retardancy action after washing process. Fig. 10(B) shows C5, C6 and C7 samples after vertical  
 645 flammability test and it confirms that PVA/20%MTP (C6) and PVA/30%MTP (C7) coatings  
 646 still have good flame retardancy action after washing the samples using tap water. The data in  
 647 Table 8 indicated that within flame application time, the flame reached the far end of C8

648 without leaving char residue. The results of horizontal and vertical flammability tests indicated  
 649 that C8 samples lost nearly all the flame retardant during washing process. In contrast, PVA in  
 650 C6 and C7 samples played an important role in fixing the flame retardant (MTP) on the cotton  
 651 fabric surface during washing process. LOI data in Table 8 confirmed the horizontal and  
 652 vertical flammability tests results. It can be seen that LOI of C8 after washing is 18.5%,  
 653 meanwhile LOI values of C5, C6 and C7 are 24.2%, 33.5% and 49.8% respectively.

654 Single flame source test data in Table 9 are also promoted the previous flammability  
 655 tests. C8 and C5 failed in single flame source test where the flame front reached the reference  
 656 mark within 60 s. In contrast, C6 and C7 pass the test and showed a higher degree of flame  
 657 retardancy compared to C8 and C5 samples. It can be concluded that PVA plays a vital role in  
 658 fixing MTP on cotton fabric surface and as the concentration of MTP in PVA/MTP mixture  
 659 increases, the flame retardancy of cotton fabric increases after washing process. Applying MTP  
 660 alone, as a coating for cotton fabric, is not sufficient to impart flame retardancy to fabric after  
 661 washing with tap water.

662  
663  
664  
665

666 **Table 9**

667 Single flame test data after washing process.

Sample code	Parameters				
	Occurrence of ignition	Whether Flame exceed 150 mm	Time to exceed 150 mm ( $t_{150}$ , s)	Ignition of filter paper	Classification
C5	Yes	Yes	50	No	Fail
C6	No	No	0	No	B,C,D,E
C7	No	No	0	No	B,C,D,E
C8	Yes	Yes	38	No	Fail

668  
669  
670  
671  
672

673 **4. Conclusions**

- 674 1- A novel single molecule intumescent flame retardant (melamine salt of tannic  
675 phosphate, MTP) was synthesized and characterized by FTIR.
- 676 2- MTP was mixed with PVA solution at 10%, 20% and 30%; and used as a coating for  
677 cotton fabrics to improve its flammability properties.
- 678 3- Horizontal flammability test data showed that coated samples C5,C6,C7 and C8 had  
679 burning rate equal to zero mm/min meanwhile the burning rate of control sample was  
680 214 mm/min
- 681 4- Vertical flammability test results indicated that applying MTP/PVA and MTP alone as  
682 coatings for cotton fabrics prohibit the flame propagation in cotton fabric samples.
- 683 5- LOI of control sample was 17.1% and it increased to 39.4%, 50.6%, 68.4% and 48.1%  
684 in C5, C6, C7 and C8 samples, respectively.
- 685 6- Single flame source test results showed that samples treated with MTP alone (C8) and  
686 PVA/MTP mixture (C5, C6 and C7) was able to pass the test and the flame did not  
687 propagate through the samples.
- 688 7- Maximum specific optical density ( $D_{s_{max}}$ ) of control sample was decreased by 79.7%,  
689 76.7%, 72.2% and 82.9% in C5, C6, C7 and C8 samples, respectively.
- 690 8- FTIR gas analyser results indicated that the coatings PVA/MTP and MTP (alone)  
691 decreased the emission of CO, CO<sub>2</sub> and HCHO gases from cotton fabrics while NH<sub>3</sub>  
692 concentrations increased due to decomposition of melamine part in MTP. The increase  
693 in NH<sub>3</sub> and H<sub>2</sub>O concentrations in the gas phase dilute the concentration of oxygen and  
694 volatile organic compounds in the combustion zone.
- 695 9- Digital photos and SEM images for char residue after smoke density test showed that  
696 MTP was able to form coherent and insulating char layer on the surface of cotton  
697 fabric. This char protected the fabric from the effect of heat and oxygen; and prevented  
698 evolving of volatile organic compounds to the combustion zone.
- 699 10- The results of LOI, horizontal flammability test, vertical flammability test, single flame  
700 source test and smoke density test confirmed that MTP (alone) and PVA/MTP mixture  
701 are more efficient as a flame retardants for cotton fabrics than the other flame retardants  
702 which consisted of PVA/TA, PVA/MP and PVA/MP/TA. Moreover, addition of TA to  
703 PVA/MP led to negative effect where the flame retardancy action of PVA/MP on cotton  
704 fabrics was better than PVA/MP/TA system.

- 705 11- FED was calculated by different models based on CO, CO<sub>2</sub>, O<sub>2</sub>, NO, NO<sub>2</sub>, HCN and  
706 HCHO concentrations. The results indicated that coated samples are less toxic than the  
707 cotton fabric sample. LC<sub>50</sub> calculations led also to the same conclusion.
- 708 12- Samples coated with PVA/MTP mixture and MTP (alone) showed antibacterial  
709 characteristic against G+ve (S.aureus) and G-ve (E-coli) bacteria. Also, as the  
710 concentration of MTP increased in coating formulation, the inhibition zone expressed in  
711 (mm) was increased.
- 712 13- Thermal analysis data indicated that PVA/MTP mixture enhanced the thermal stability  
713 of cotton fabric at high temperature ( $T_{50\%}$ ) and increased the char residue at 750 °C  
714 from 0.3% in control sample to 25.5% in C7 sample.
- 715 14- Durability studies showed that cotton samples coated with PVA/20%MTP (C6) and  
716 PVA/30%MTP (C7) can maintain good flame retardancy action after washing them  
717 with tap water. In contrast, C8 sample lost its flame retardancy due to losing MTP  
718 particles during washing process. This indicated that PVA played an important role in  
719 preserving MTP on cotton samples during washing process.

720

721

722

723

724

725

726

727

728

729

730

731

732

733

734

735

736

737

738

740 **References**

- 741 Abdelkhalik, A., Makhlof, G., Hassan, M.A., 2019. Manufacturing, thermal stability, and  
742 flammability properties of polypropylene containing new single molecule intumescent flame  
743 retardant. *Polym. Adv. Technol.* 30, 1403-1414. <https://doi.org/10.1002/pat.4573>
- 744 ASTM D6413: 2015. Standard test method for flame resistance of textiles (vertical test).
- 745 Carosio, F., Negrell-Guirao, C., Blasio, A.D., Alongi, J., David, G., Camino, G., 2015. Tunable  
746 thermal and flame response of phosphonated oligoallylamines layer by layer assemblies on  
747 cotton. *Carbohydr. Polym.* 115, 752-759. <https://doi.org/10.1016/j.carbpol.2014.06.066>
- 748 Chan, S.Y., Si, L., Lee, K.I., Ng, P.F., Chen, L., Yu, B., Hu, Y., Yuen, R.K.K., Xin, J.H., Fei,  
749 B., 2018. A novel boron–nitrogen intumescent flame retardant coating on cotton with improved  
750 washing durability. *Cellulose* . 25, 843- 857. <https://doi.org/10.1007/s10570-017-1577-2>
- 751 Chen, Y., Wang, Q., 2007. Reaction of melamine phosphate with pentaerythritol and its  
752 products for flame retardation of polypropylene. *Polym. Adv. Technol.* 18(8), 587-600.
- 753 Chen, Y., Wan, C., Liu, S., Wang, P., Zhang, G., 2021. A novel flame retardant based on  
754 polyhydric alcohols and P–N synergy for treatment of cotton fabrics. *Cellulose*.  
755 <https://doi.org/10.1007/s10570-020-03615-7>
- 756 Chen, Y., Wang, D., Liu, S., Lu, Y., Zhang, G., Zhang, F., 2020. A novel P–N-based flame  
757 retardant with multi-reactive groups for treatment of cotton fabrics. *Cellulose*. 27, 9075–9089.  
758 <https://doi.org/10.1007/s10570-020-03387-0>
- 759 Chow, C.L., Han, S.S., Han, G.Y., Hou, G.L., Chow, W.K., 2020. Assessing smoke toxicity of  
760 burning combustibles by four expressions for fractional effective dose. *Fire. Mater.* 44, 804–  
761 813. <https://doi.org/10.1002/fam.2875>
- 762 Chung, C., Lee, M., Choe, E. K., 2004. Characterization of cotton fabric scouring by FT-IR  
763 ATR spectroscopy. *Carbohydr. Polym.* 58, 417–420.
- 764 Dayanand, C., Bhikshamaiah, G., Tyagaraju, V.J., Salagram, M., Murthy, A.S.R.K., 1996.  
765 Structural investigations of phosphate glasses: a detailed infrared study of the  $x(\text{PbO})-(1-$   
766  $x)\text{P}_2\text{O}_5$  vitreous system. *J. Mater. Sci.* 31, 1945-1967.
- 767 Das, A.K., Islam, M.N., Faruk, M.O., Ashaduzzaman, M., Dungani, R., Rosamah, E., Hartati,  
768 S., Rumidatul, A., 2020. Hardwood tannin: sources, utilizations, and prospects, in: Aires, A.  
769 (Eds.), *tannins structural properties, biological properties and current knowledge*. IntechOpen  
770 Limited, London, pp. 1-18.

771 Dong, S., Wu, F., Chen, L., Wang, Y., Chen, S., 2016. Preparation and characterization of  
772 Poly(vinyl alcohol)/graphene nanocomposite with enhanced thermal stability using PETVIm-Br  
773 as stabilizer and compatibilizer. *Polym. Degrad. Stab.* 131, 42-52.

774 Fang, F., Zhang, X., Meng, Y., Gu, Z., Bao, C., Ding, X., Li, S., Chen, X., Tian, X., 2015.  
775 Intumescent flame-retardant coatings on cotton fabric of chitosan and ammonium  
776 polyphosphate via layer-by-layer assembly. *Surf. Coat. Technol.* 262, 9-14.  
777 <https://doi.org/10.1016/j.surfcoat.2014.11.011>

778 Gaikwad, K.K., Lee, J.Y., Lee, Y.S., 2015. Development of polyvinyl alcohol and apple  
779 pomace bio-composite film with antioxidant properties for active food packaging application.  
780 *J. Food. Sci. Technol.* 53(3), 1608-1619.

781 Galletti, G.C., Reeves, J.B., 1992. Pyrolysis/gas chromatography/ion-trap detection of  
782 polyphenols (vegetable tannins): preliminary results. *Org. Mass. Spectrom.* 27, 226–230.

783 Hassan, M., Nour, M., Abdelmonem, Y., Makhlof, G., Abdelkhalik, A., 2016. Synergistic  
784 effect of chitosan-based flame retardant and modified clay on the flammability properties of  
785 LLDPE. *Polym. Degrad. Stab.* 133, 8-15.  
786 <https://doi.org/10.1016/j.polymdegradstab.2016.07.011>

787 Hu, S., Tan, Z.W., Chen, F., Li, J.G., Shen, Q., Huang, Z.X., Zhang, L.M., 2020. Flame-  
788 retardant properties and synergistic effect of ammonium polyphosphate/aluminum  
789 hydroxide/mica/silicone rubber composites. *Fire. Mater.* 44, 673–682.  
790 <https://doi.org/10.1002/fam.2831>

791 ISO 13344: 1996. Determination of the lethal toxic potency of fire effluents.  
792 ISO/FDIS 13344: 2015. Estimation of the lethal toxic potency of fire effluents.

793 ISO 3795: 1989. Road vehicles, and tractors and machinery for agriculture and forestry —  
794 Determination of burning behaviour of interior materials.

795 ISO 11925-2:2020. Reaction to fire tests — Ignitability of products subjected to direct  
796 impingement of flame — Part 2: Single-flame source test.

797 ISO 4589-2:2017. Plastics — Determination of burning behaviour by oxygen index — Part 2:  
798 Ambient-temperature test.

799 ISO 5659-2:2017. Plastics — Smoke generation — Part 2: Determination of optical density by  
800 a single-chamber test.

801 ISO 13934-1:2013. Textiles — Tensile properties of fabrics — Part 1: Determination of  
802 maximum force and elongation at maximum force using the strip method.

803 BS EN 13501-1:2018. Fire classification of construction products and building elements.  
804 Classification using data from reaction to fire tests.

805 Jian, R., Ai, Y., Xia, L., Zhao, L., Zhao, H., 2019. Single component phosphamide-based  
806 intumescent flame retardant with potential reactivity towards low flammability and smoke  
807 epoxy resins. *J. Hazard. Mater.* 371, 529–539.

808 Laoutid, F., Bonnaud, L., Alexandre, M., Lopez-Cuesta, J.M., Dubois, P., 2009. New prospects  
809 in flame retardant polymer materials: from fundamentals to nanocomposites. *Mater. Sci. Eng.*  
810 *R. Rep.* 63, 100–125. <https://doi.org/10.1016/j.mser.2008.09.002>

811 Levchik, S.V., Levchik, G.F., Balabanovich, A.I., Camino, G., Costa, L., 1996. Mechanistic  
812 study of combustion performance and thermal decomposition behaviour of nylon 6 with added  
813 halogen-free fire retardants. *Polym. Degrad. Stab.* 54; 217–222. <https://doi.org/10.1016/s0141->  
814 [3910\(96\)00046-8](https://doi.org/10.1016/s0141-3910(96)00046-8)

815 Makhlof, G., Abdelkhalik, A., Hassan, M.A., 2020. Combustion toxicity of polypropylene  
816 containing melamine salt of pentaerythritol phosphate with high efficiency and stable flame  
817 retardancy performance. *Process. Saf. Environ. Prot.* 138, 300-311.  
818 <https://doi.org/10.1016/j.psep.2020.04.012>

819 Makhlof, G., Hassan, M., Nour, M., Abdelmonem, Y., Abdelkhalik, A., 2017a. Evaluation of  
820 fire performance of linear low-density polyethylene containing novel intumescent flame  
821 retardant. *J. Therm. Anal. Calorim.* 130 (2), 1031–1041. DOI 10.1007/s10973-017-6418-x

822 Makhlof, G., Hassan, M., Nour, M., Abdelmonem, Y., Abdelkhalik, A., 2017b. A novel  
823 intumescent flame retardant: synthesis and its application for linear low-density polyethylene.  
824 *Arab. J. Sci. Eng.* 42 (10), 4339–4349. DOI 10.1007/s13369-017-2443-0

825 Nam, S., Condon, B.D., Xia, Z., Nagarajan, R., Hinchliffe, D.J., Madison, C.A., 2017.  
826 Intumescent flame-retardant cotton produced by tannic acid and sodium hydroxide. *J. Anal.*  
827 *Appl. Pyrolysis.* 126, 239-246. <https://doi.org/10.1016/j.jaap.2017.06.003>

828 Pan, H., Wang, W., Pan, Y., Zeng, W., Zhan, J., Song, L., Hu, Y., Liew, K. M., 2015.  
829 Construction of layer-by-layer assembled chitosan/titanate nanotubes based nanocoating on  
830 cotton fabrics: flame retardant performance and combustion behaviour. *Cellulose.* 22, 911-923.  
831 <https://doi.org/10.1007/s10570-014-0536-4>

832 Pantoja-Castro, M.A., González-Rodríguez, H., 2011. Study by infrared spectroscopy and  
833 thermogravimetric analysis of tannins and tannic acid. *Rev. Latinoamer. Quím.* 39 (3), 107-  
834 112.

835 Ramakrishnan, K., Krishnan, M.R.V., 1994. Tannin—Classification, analysis and applications.  
836 *Anc. Sci. Life.* XIII(3-4), 232-238.

837 Singh, A.P, and Kumar, S., 2020. Applications of tannins in industry, in: Aires, A. (Eds.),  
838 Tannins structural properties, biological properties and current knowledge. IntechOpen  
839 Limited, London, pp. 1-19.

840 Stec, A.A., 2017. Fire toxicity – The elephant in the room? *Fire. Saf. J.* 91, 79-90.  
841 <https://doi.org/10.1016/j.firesaf.2017.05.003>

842 Stull, J.O., 2008. U.S. Fire Administration Firefighter Autopsy Protocol, Federal Emergency  
843 Management Agency.

844 Tributsch, H., and Fiechter, S., 2008. The material strategy of fire-resistant tree barks, in: De  
845 Wilde, W.P., Brebbia, C.A. (Eds.), High performance structures and materials IV. WIT Press  
846 Southampton, Boston, pp. 43-52.

847 Van der Veen, I., de Boer, J., 2012. Phosphorus flame retardants: Properties, production,  
848 environmental occurrence, toxicity and analysis. *Chemosphere.* 88, 1119–1153. [https://doi.org/](https://doi.org/10.1016/j.chemosphere.2012.03.067)  
849 [10.1016/j.chemosphere.2012.03.067](https://doi.org/10.1016/j.chemosphere.2012.03.067)

850 Viswanath, V., Leo, V.V., Prabha, S.S., Prabhakumari, C., Potty, V.P., Jisha, M.S., 2015.  
851 Thermal properties of tannin extracted from *Anacardium occidentale* L. using TGA and FT-IR  
852 spectroscopy. *Nat. Prod. Res.* 30 (2), 223-227. DOI: 10.1080/14786419.2015.1040992

853 Wan, C., Liu, M., Tian, P., Zhang, G., Zhang, F., 2020. Renewable vitamin B5 reactive N–P  
854 flame retardant endows cotton with excellent fire resistance and durability. *Cellulose.* 27;  
855 1745–1761. <https://doi.org/10.1007/s10570-019-02886-z>

856 Wang, D., Ma, J., Liu, J., Tian, A., Fu, S., 2021. Intumescent flame-retardant and ultraviolet-  
857 blocking coating screen-printed on cotton fabric. *Cellulose.* [https://doi.org/10.1007/s10570-](https://doi.org/10.1007/s10570-020-03669-7)  
858 [020-03669-7](https://doi.org/10.1007/s10570-020-03669-7)

859 Wahyono, T., Astuti, D.A., Wiryawan, I.K.G., Sugoro, I., Jayanegara, A., 2019. Fourier  
860 transform mid-infrared (FTIR) spectroscopy to identify tannin compounds in the panicle of  
861 sorghum mutant lines. *IOP Conf. Ser.: Mater. Sci. Eng.* 546, 042045. doi:10.1088/1757-  
862 899X/546/4/042045

863 Xia, Z., Singh, A., Kiratitanavit, W., Mosurkal, R., Kumar, J., Nagarajan, R., 2015. Unraveling  
864 the mechanism of thermal and thermo-oxidative degradation of tannic acid. *Thermochim.*  
865 *Acta.* 605, 77–85.

866 Xu, F., Zhong, L., Xu, Y., Zhang, C., Zhang, F.X., Zhang, G.X., 2019. Highly efficient flame-  
867 retardant and soft cotton fabric prepared by a novel reactive flame retardant. *Cellulose* 26;  
868 4225–4240. <https://doi.org/10.1007/s10570-019-02374-4>

869 Yang, B., Chen, Y., Zhang, M., Yuan, G., 2019. Synergistic and compatibilizing effect of  
870 octavinyl polyhedral oligomeric silsesquioxane nanoparticles in polypropylene/intumescent  
871 flame retardant composite system. *Compos. A. Appl. Sci. Manuf.* 123, 46–58.  
872 <http://dx.doi.org/10.1016/j.compositesa, 2019.04.032>.

873 Zhu, W.J., Yang, M.Y., Huang, H., Dai, Z., Cheng, B.W., Hao, S.S., 2020a. A phytic acid-  
874 based chelating coordination embedding structure of phosphorus-boron-nitride synergistic  
875 flame retardant to enhance durability and flame retardancy of cotton. *Cellulose*. 27, 4817–  
876 4829. <https://doi.org/10.1007/s10570-020-03063-3>

877 Zaikov, G.E., Lomakin, S.M., 1998. Flame retardants: poly(vinyl alcohol) and silicon  
878 compounds. In: Pritchard, G., (eds.) *Plastic Additives. Polymer Science and Technology*  
879 *Series*, pp. 55-56. Springer, Dordrecht (1998).

880 Zhu, X.K., Pang, H.C., Zheng, N., Tian, P., Ning, G.L., 2020b. High effects of smoke  
881 suppression and char formation of Ni-Mo/ Mg(OH)<sub>2</sub> for polypropylene. *Polym. Adv. Technol.*  
882 31, 1688–1698. <https://doi.org/10.1002/pat.4896>

883

# Figures



Figure 1

(A) Schematic illustration of a suggested synthetic route of MTP; (B) the structure of cotton fabric/PVA/MTP prepared by dip-pad-dry method.

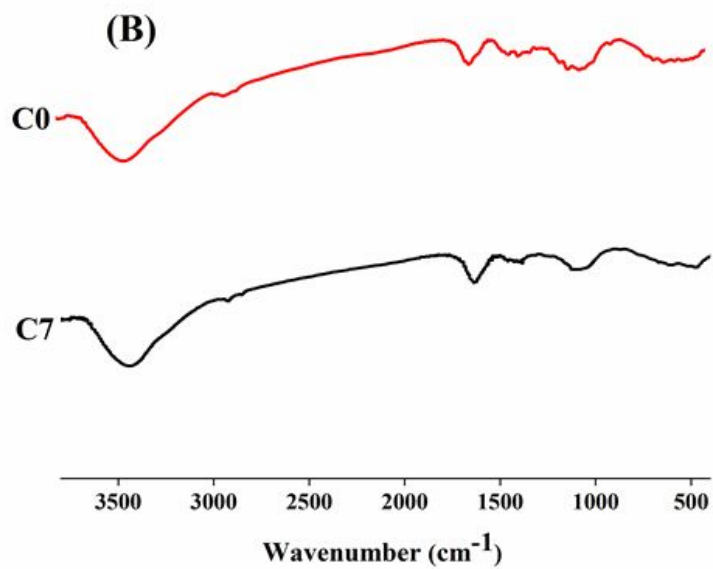
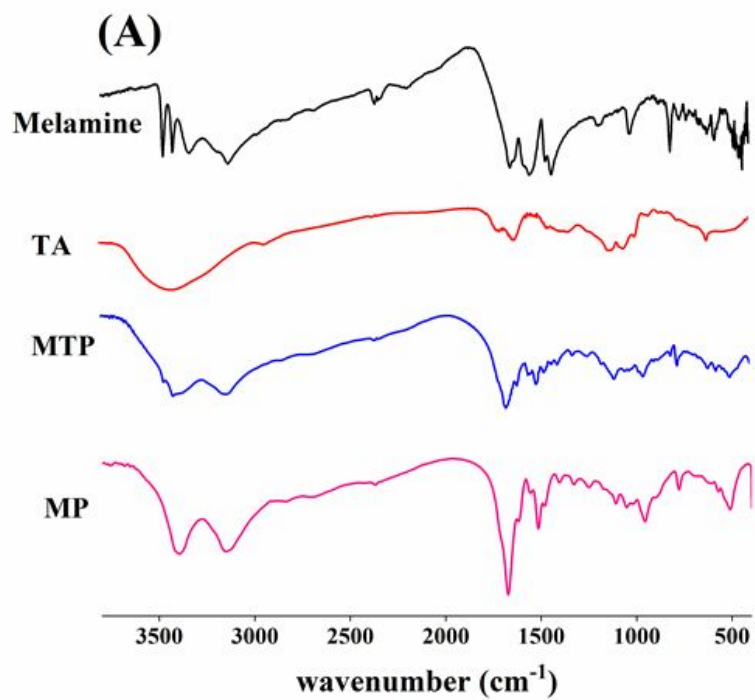


**Figure 2**

(A) FTIR spectra of melamine, MP, TA and MTP; (B) FTIR spectra of C0 and C7.

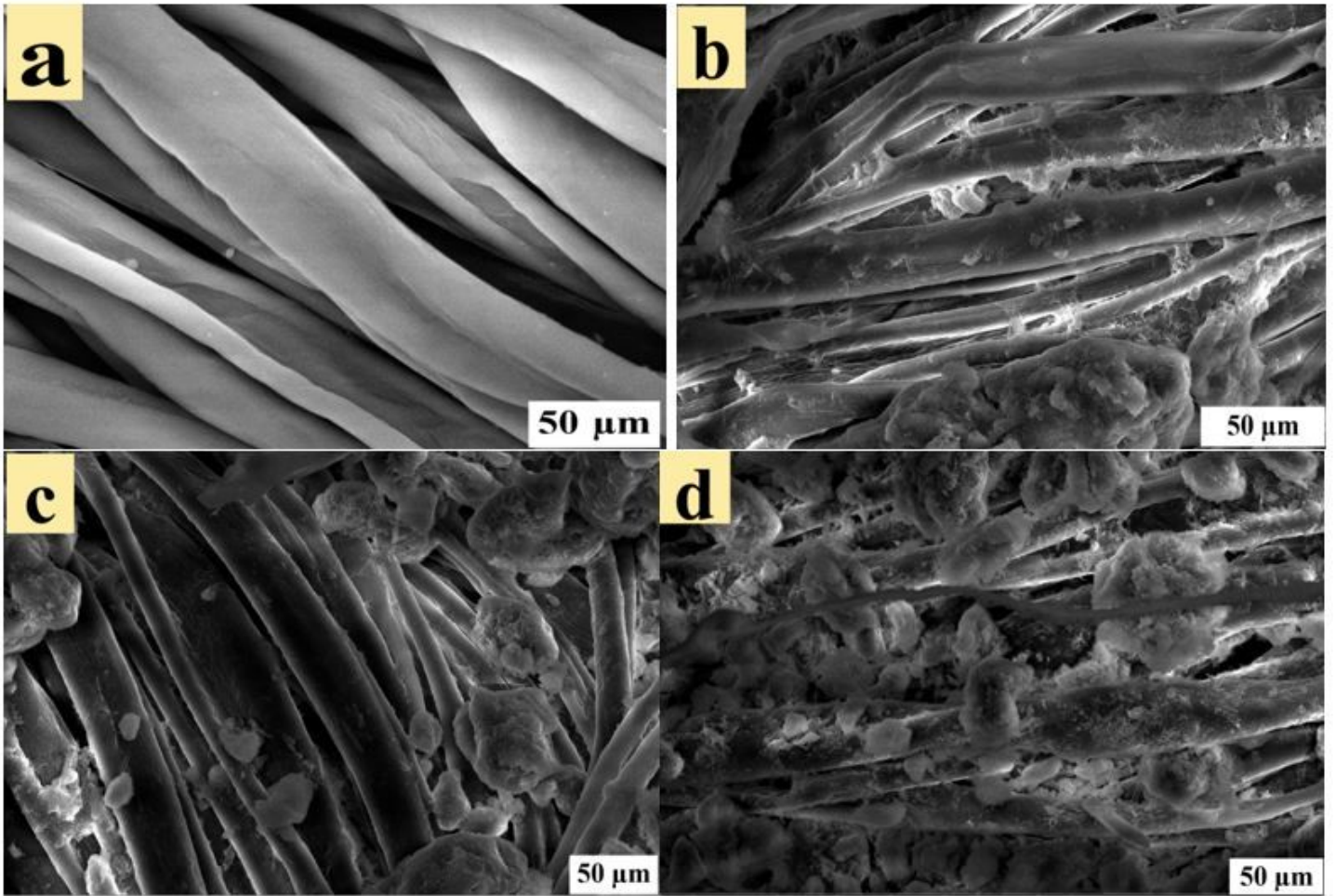


**Figure 3**

(a-d) The surface morphology of C0, C5, C7 and C8, respectively.

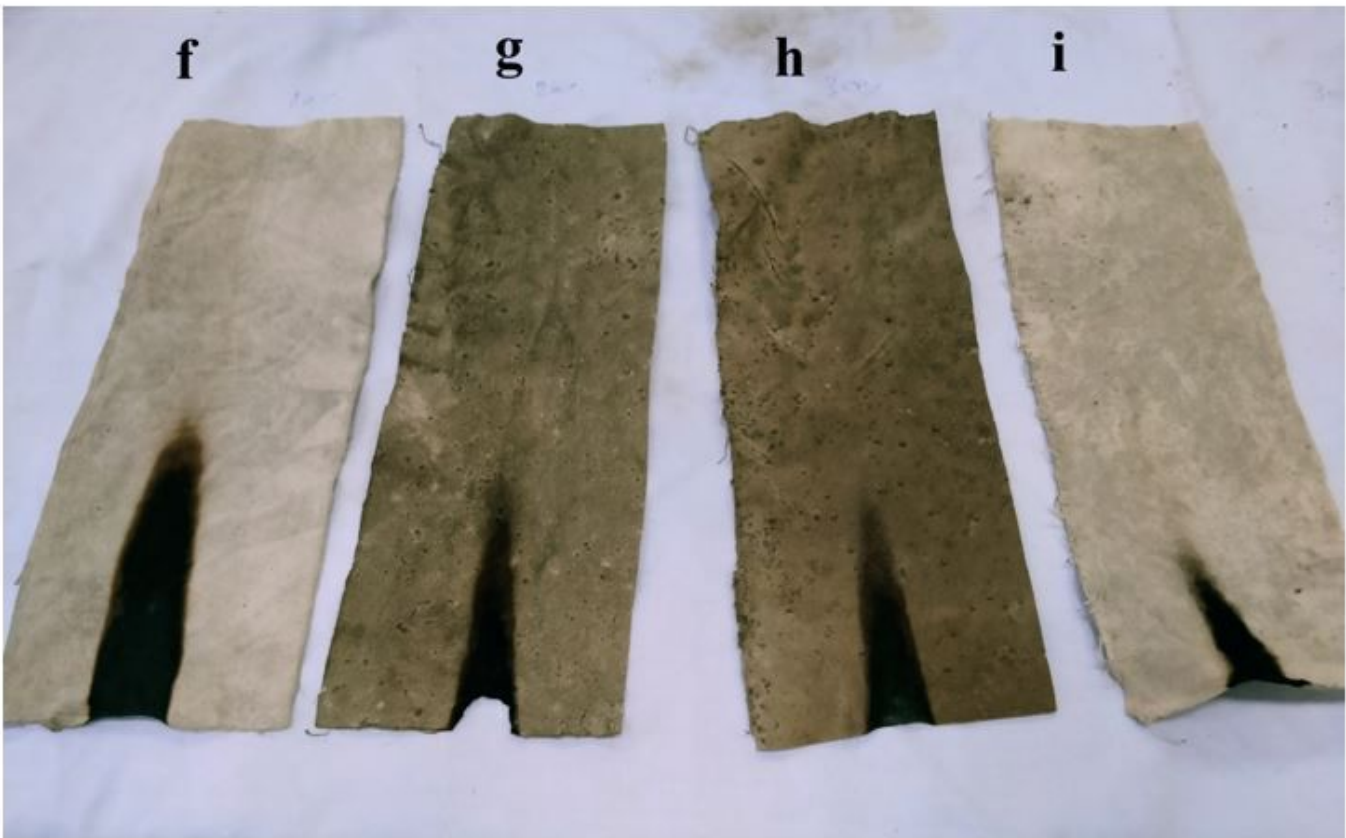
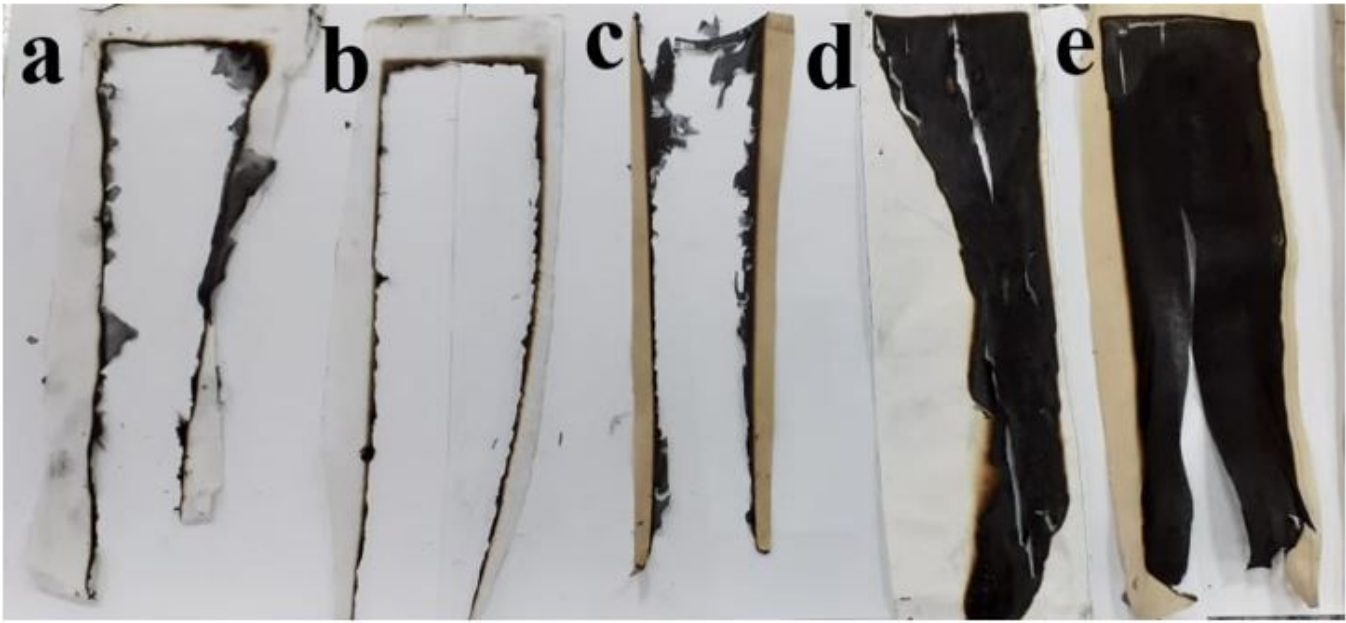


**Figure 4**

(a-i) Digital photographs for control and treated samples after vertical flammability test.

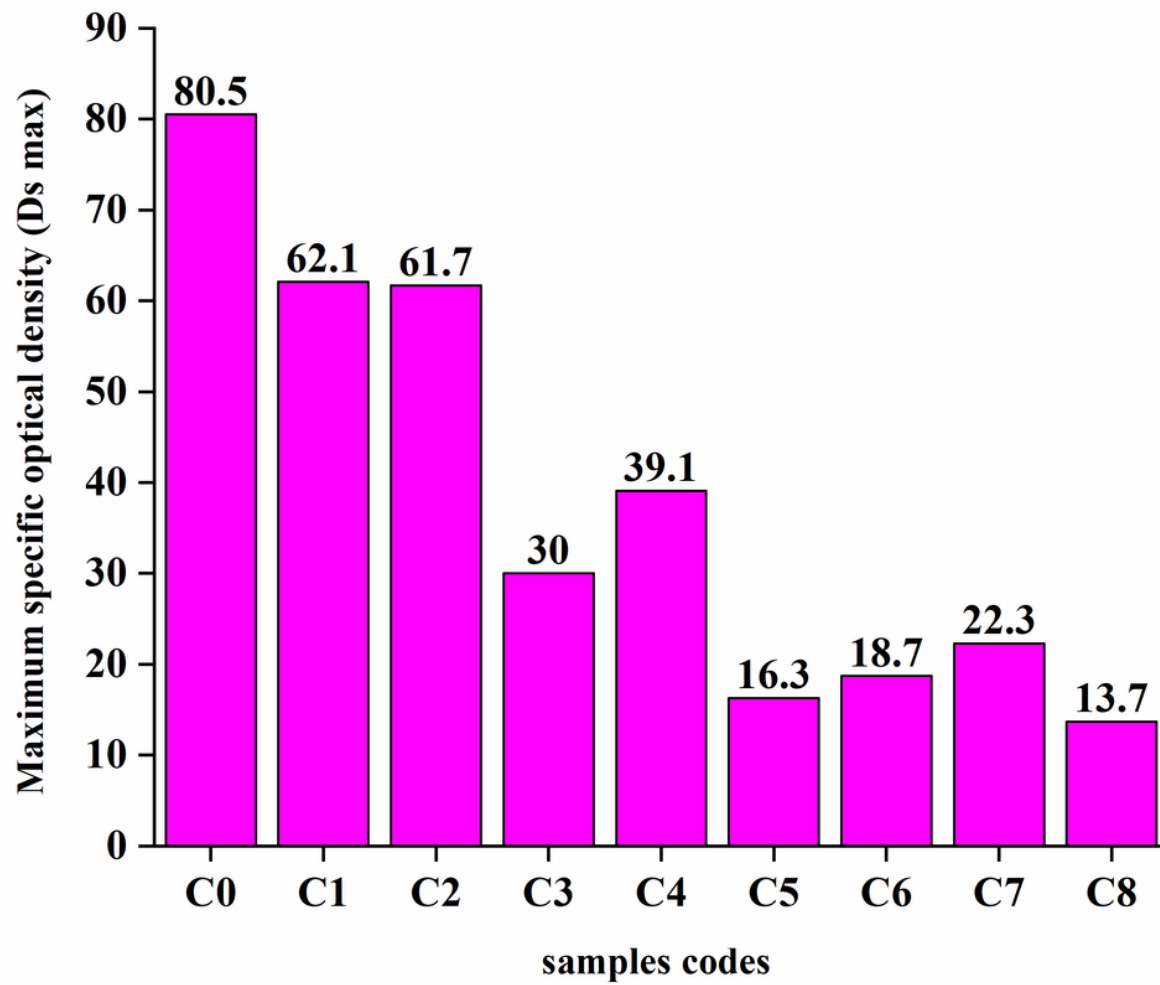


Figure 5

Values of maximum specific optical density (Dsmax) for control and coated samples.

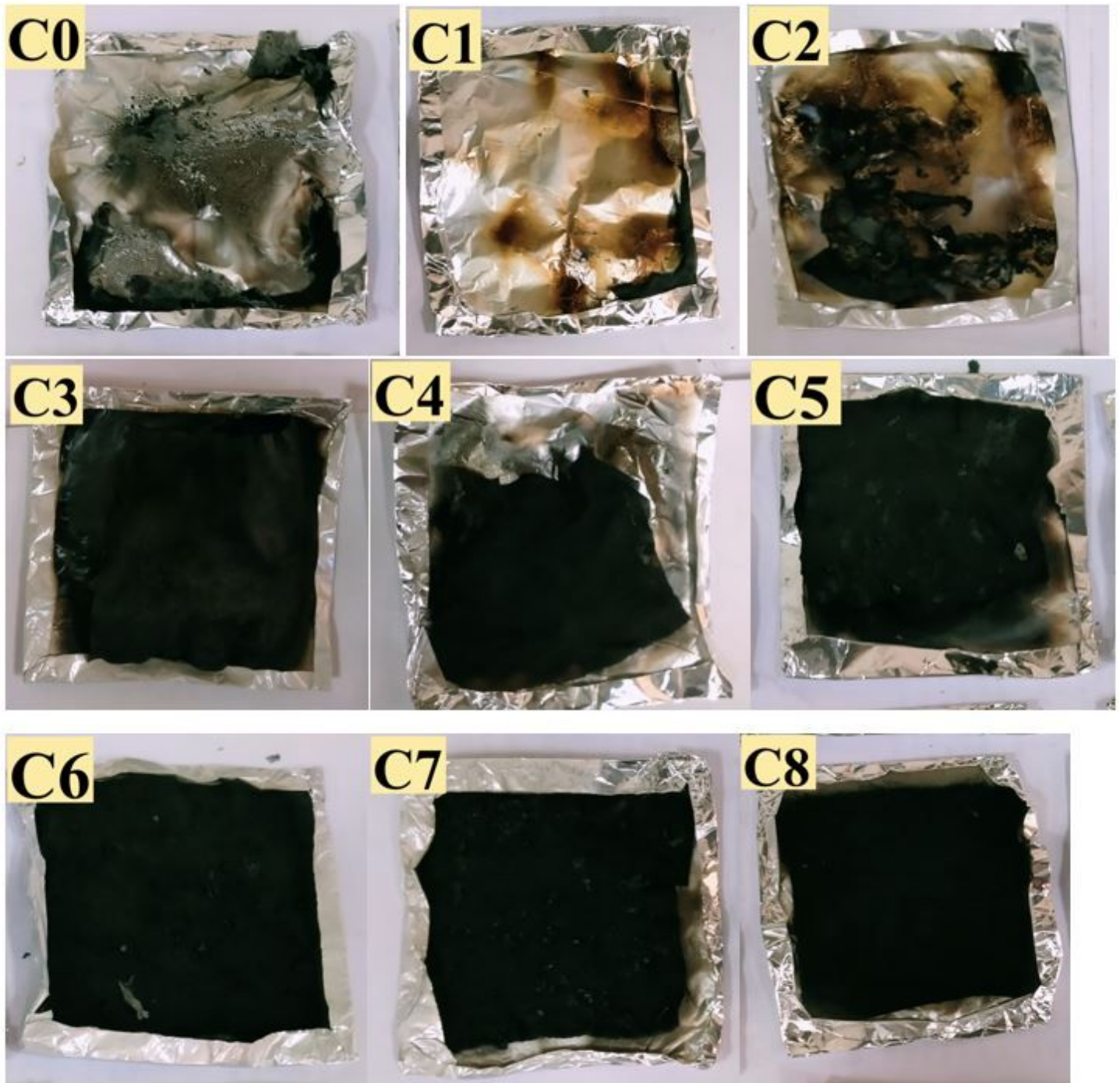
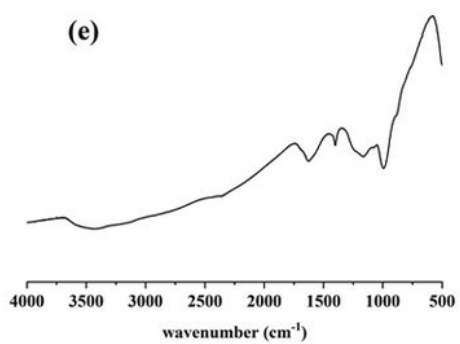
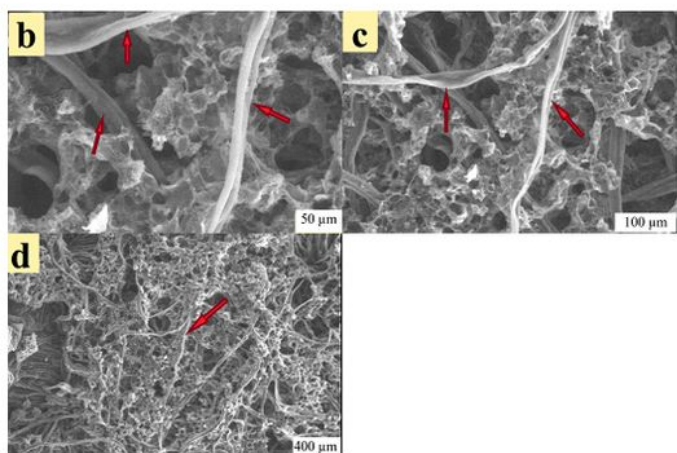
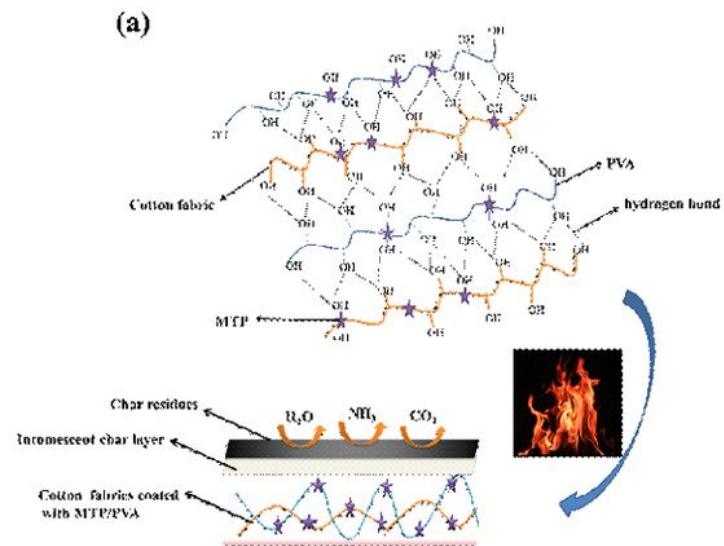


Figure 6

Digital photographs of control and treated samples after smoke density test.



**Figure 7**

(a) Schematic illustration of a possible flame retardant mechanism for cotton fabrics treated with PVA/MTP during combustion; (b-d) SEM images for char residue formed after smoke density test of C7; (e) FTIR analysis of char residue of C7 after smoke density test.

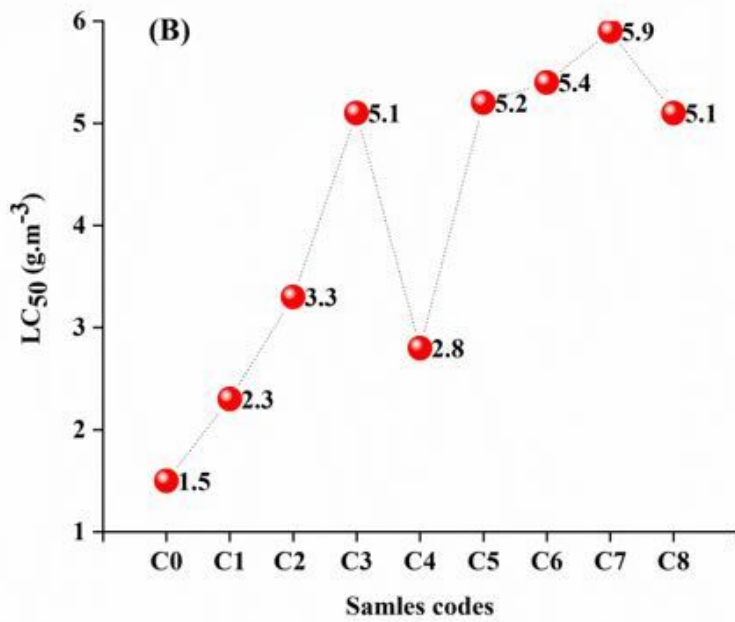
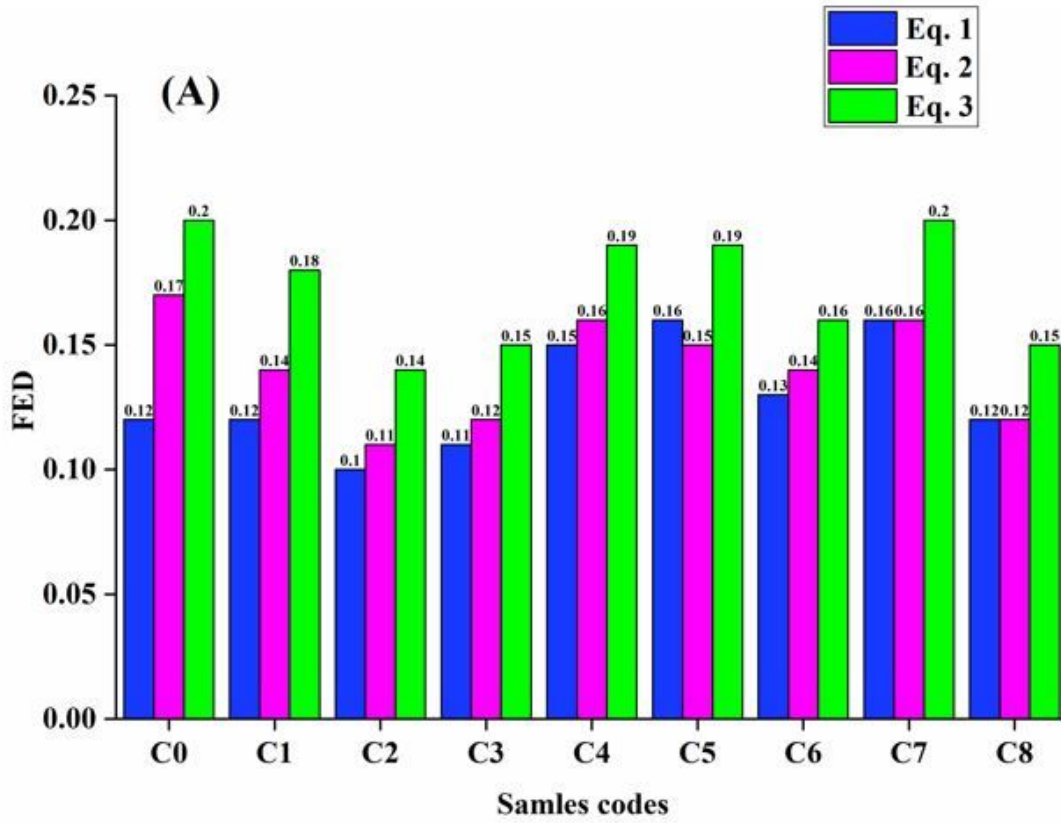
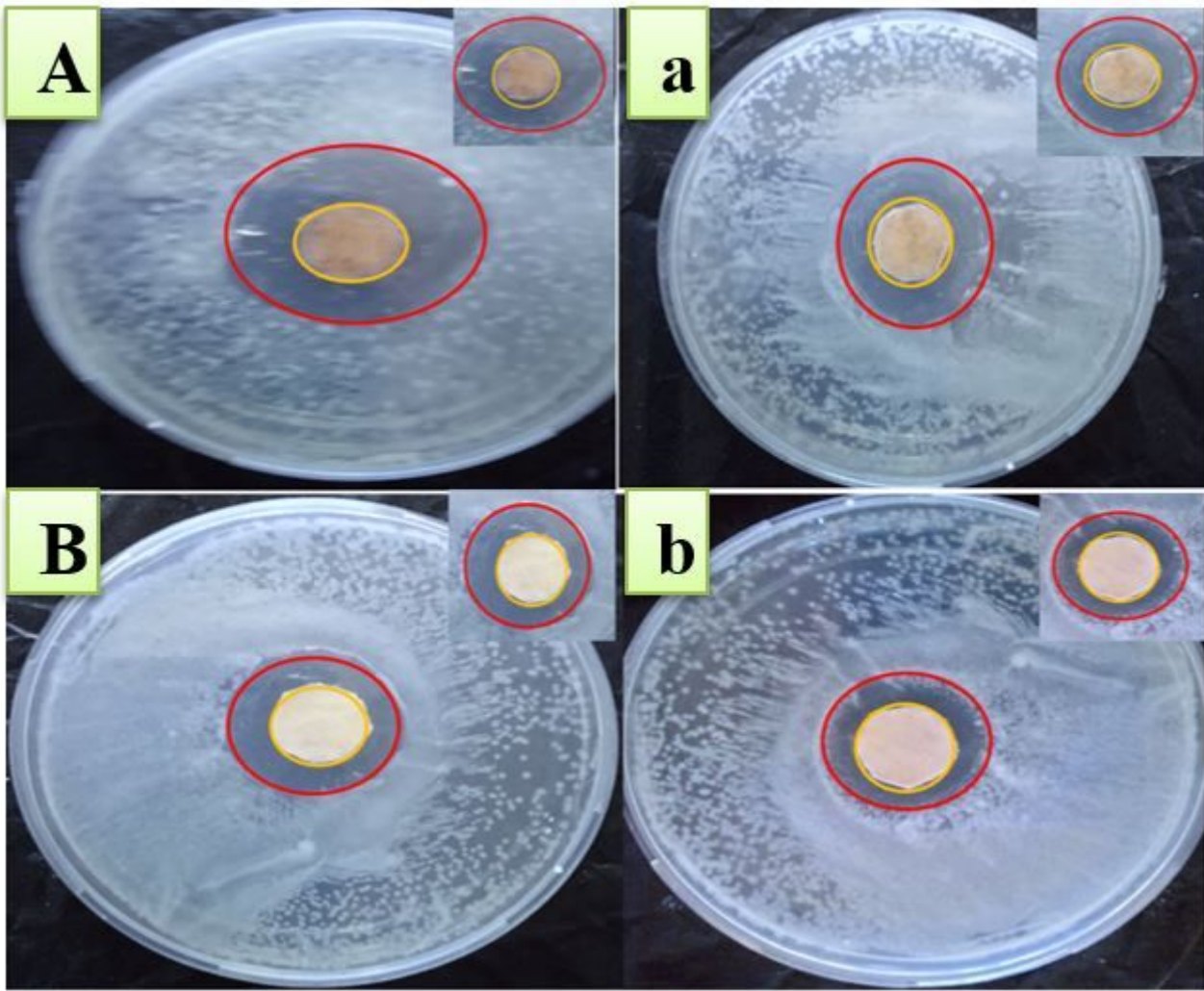


Figure 8

(A) FED and (B) LC<sub>50</sub> values of control and treated samples.



**Figure 9**

(A,B) digital photographs for zone of inhibition formed by *S.aureus* in C7 and C8 respectively; and (a,b) digital photographs for zone of inhibition formed by *E. coli* in C7 and C8, respectively.

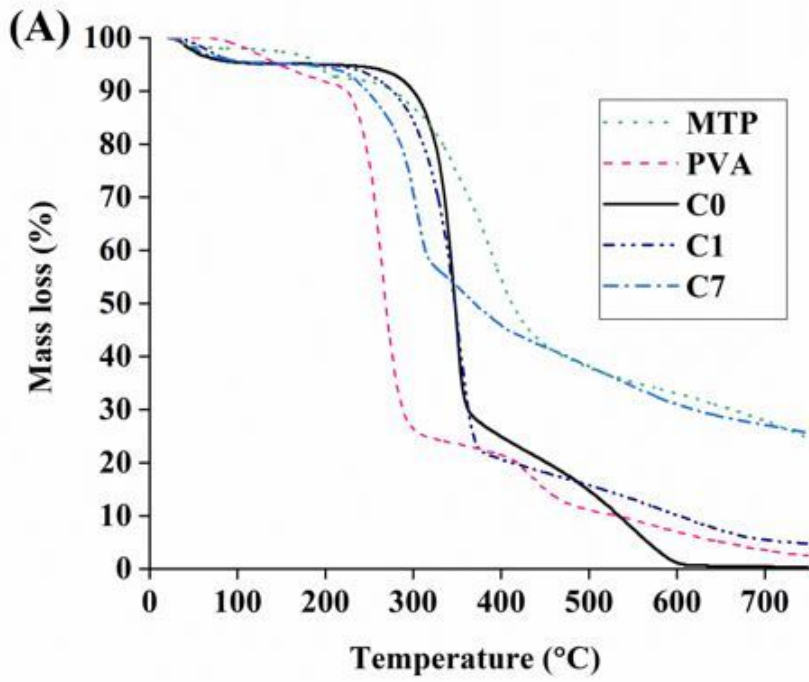


**Figure 10**

(A) TGA curves of MTP, PVA, C0, C1 and C7; (B) Digital photographs of C7, C6 and C5 samples after washing and performing vertical flammability test.